Enabling Nanopore for Sensing Individual Amino Acids by a Derivatization Strategy

Xiaojun Wei[1,2‖], Dumei Ma[3,5‖], Lihong Jing[4*], Leon Y. Wang[2§], Xiaoqin Wang[2], Zehui Zhang[1], Brian J. Lenhart[2], Yingwu Yin[5], Qian Wang[3*], and Chang Liu[1,2*]

[1]Biomedical Engineering Program, University of South Carolina, Columbia, SC 20208, USA

[2]Department of Chemical Engineering, University of South Carolina, Columbia, SC 29208, USA

[3]Department of Chemistry and Biochemistry, University of South Carolina, Columbia, SC 29208, USA

[4]Key Laboratory of Colloid, Interface and Chemical Thermodynamics, Institute of Chemistry, Chinese Academy of Sciences, Bei Yi Jie 2, Zhong Guan Cun, Beijing 100190, China

[5]Department of Chemical and Biochemical Engineering, College of Chemistry and Chemical Engineering, Xiamen University, Xiamen 361005, Fujian, China

[‖]These authors contributed equally to this work.

[§]Present address: Dreher High School, 3319 Millwood Ave, Columbia, SC 29205, USA

[*]Address correspondence to: changliu@cec.sc.edu, wang263@mailbox.sc.edu, jinglh@iccas.ac.cn

Experiment Section

Materials. Naphthalene isothiocyanate (NITC) and all amino acids were purchased from Sigma-Aldrich and used without further purification. The derivative reagent 2,3-naphthalenedicarboxaldehyde (NDA) was synthesized according to the reference method (*Mallouli, A. et al. Synthesis-Stuttgart 1980, 689*). The KCl working solution was prepared using deionized water from a Milli-Q water purification system (resistivity of 18.2 MΩ/cm, 25°C, Millipore Corporation) and was filtered through 0.02 μm filter before use. α-HL from Staphylococcus aureus (lyophilized powder, Protein ~60 % by Lowry, ≥10,000 units/mg protein) was purchased from Sigma-Alrich.

General procedure for preparing of NDA derivatives. NDA derivatives were synthesized according to the route I as shown in Fig. S1. NDA (0.7 mmol), amino acid (0.6mmol), trifluoroacetate (0.8 mmol) and acetonitrile (10 mL) were stirred under reflux condition for 3 h. The precipitate was washed with acetonitrile to afford the corresponding products. The average yields are 60-82 %.

General procedure for preparing of NITC derivatives. NITC derivatives were synthesized according to the route II as shown in Fig. S1. NITC (1 mmol), amino acid (1.1 mmol), Na_2CO_3 (0.1 M, 4 mL) and acetonitrile (8 mL) under reflux condition overnight. The resulting precipitate was collected, washed with 1 M HCl and Methanol, and dried to afford the corresponding products. The average yields are 80-89 %.

Characterization of amino acid derivatives. The ^{1}H and ^{13}C NMR spectra were recorded at 298 K in deuterated solvents using Bruker Avance 400 MHz spectrometer. Data is represented as follows: chemical shift, multiplicity (s = singlet, d= doublet, t = triplet, q = quartet, m = multiplet), coupling constants in Hertz (Hz), integration.

Nanopore fabrication and low-noise electrical recording. All electrophysiology experiments were performed on the Planar Lipid Bilayer workstation (Warner Instruments) at room temperature

(~23°C). Fabrication of α-HL nanopore devices follows traditional method previously reported. Briefly, an orifice (200 μm in diameter) punctured on a 25 μm thick Delrin wall that separates the *cis* (grounded) and the *trans* chambers of the flow cell was precoated with 1:10 hexadecane/pentane (Sigma-Aldrich). Then both chambers were filled with 1 mL of 3 M KCl solution buffered in 10 mM Tris-HCl (pH 8). To form a lipid bilayer membrane in the orifice, 20 μL (10 mg/mL) 1,2 diphytanoyl-sn-glycero-3-phosphocholine (Avanti Polar Lipids) dissolved in pentane (Sigma-Aldrich) was added to the *cis* side of chambers to allow self-assembly. Following this, electrical potential was applied to the *trans* side using Ag/AgCl electrodes and slowly ramped up to examine the stability of the membrane at ± 200 mV. The membrane capacitance was maintained between 160-170 pF with various voltage bias values throughout each experiment.

To insert a single nanopore channel into the lipid bilayer, *trans* voltage was changed to 100 mV and a small amount (~0.05 μg) of α-HL protein (Sigma-Aldrich) were added from a monomeric stock solution made in 3 M KCl to the *cis* compartment. To ensure consistency of testing conditions, the direction of each α-HL nanopore was examined by comparing the value of the channel current under positive and negative voltages after its insertion into the lipid bilayer. A properly inserted α-HL pore exhibits larger ionic current under a positive *trans* voltage than it is under a negative voltage. After a stable α-HL protein nanopore was inserted and confirmed by an open pore current, an analyte was added to the *cis* chamber at a bulk concentration of 200 μM from a 10 mM stock solution made in DMSO.

Data collection and analysis. Ionic current recordings were collected using a patch clamp amplifier (Warner Instruments) with a built-in high-pass Bessel filter (cutoff: 5 kHz) at a holding potential of 100 mV. After sample addition to the *cis* chamber, magnetic stirring was used to disperse the sample before characteristic signal was recorded. Each sample was measured in three replicates with a 30 min total duration. The ionic current was sampled at 100 kHz using a Digidata 1440A analog-

to-digital converter (Molecular Devices) and processed with pClamp10 software (Molecular Devices). A fresh α-HL protein nanopore was used for each replicate. The raw data was analyzed using an in-house Matlab based algorithm to find the current blockade and the dwell time of each eligible event, which are two commonly used properties for discriminating different molecules when they translocate nanopores. Results processed by the Matlab algorithm were confirmed by manual inspection.

Molecular modeling. Geometry optimization of amino acids and their derivatives was calculated using Q-chem 4.3 (*Shao, Y. H. et al. Molecular Physics 2015, 113, 184*). Unrestricted B3LYP functional was employed to describe our system, making use of the 6-31++G basis sets for C, H, O, N and S atoms. Solvent effects (KCl aqueous solution with a dielectric constant of 55) were included using the PCM implicit solvation model. The VDW radius of calculated by Multiwfn program (*Lu, T. et al. Journal of Computational Chemistry 2012, 33, 580*), in which VDW surface is defined by the lengths of the three sides of the cube. The results were shown in Table S1.

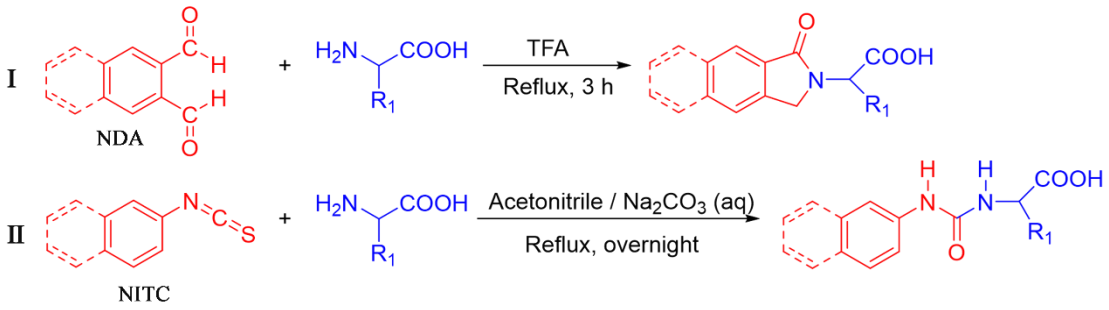

Fig. S1 Synthetic routes of different amino acid derivatives. Route I is for NDA derivatives and route II is for NITC derivatives.

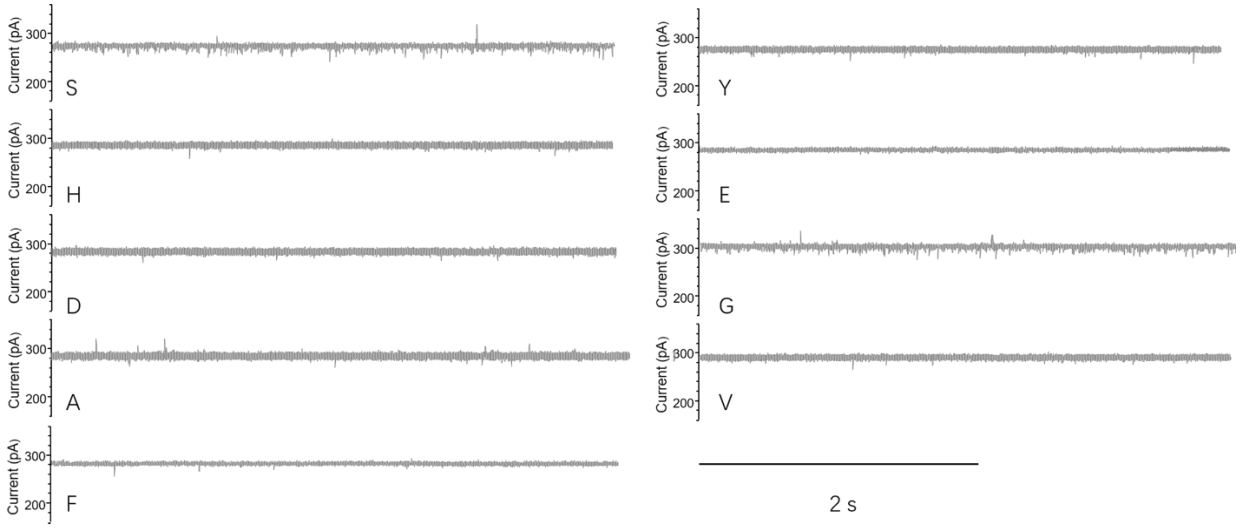

Fig. S2 Representative translocation current trace of the bare amino acids through α-HL nanopores (final concentration 200 μM). Data were acquired in a buffer of 3 M KCl and 10 mM Tris (pH 8.0) with the transmembrane potential held at +100 mV.

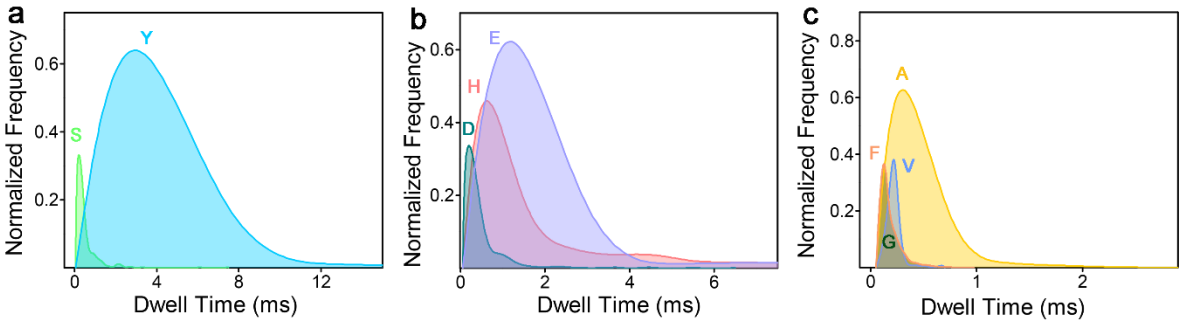

Fig. S3 Typical superimposed histograms of events per bin of dwell time for different NITC derivatives, analyzed individually and grouped according to the properties of amino acids: (a) polar, (b) charged and (c) non-polar.

Table S1 The molecular structures and space-filling structures of selected amino acids derivatized with NDA and NITC, respectively. Results obtained by molecular modeling with Q-chem 4.3 software.

			NDA	space-filling structure of NDA derivatives	NITC	space-filling structure of NITC derivatives
None Polar	Gly	G	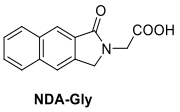 NDA-Gly	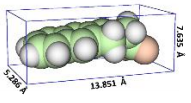	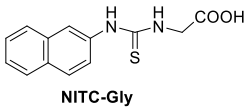 NITC-Gly	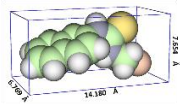
	Ala	A	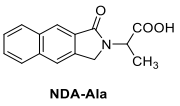 NDA-Ala	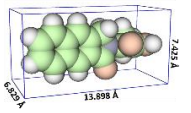	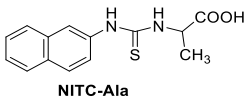 NITC-Ala	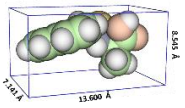
	Val	V	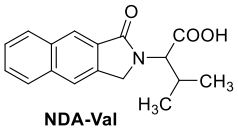 NDA-Val	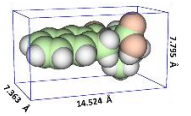	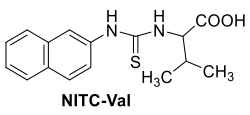 NITC-Val	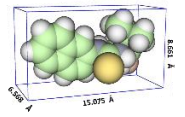
	Phe	F	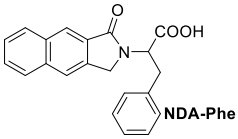 NDA-Phe	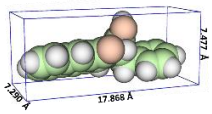	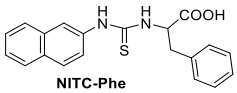 NITC-Phe	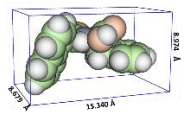
Polar	Ser	S	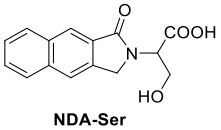 NDA-Ser	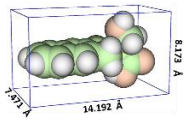	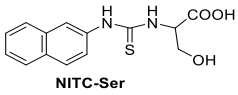 NITC-Ser	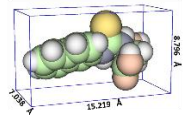
	Tyr	Y	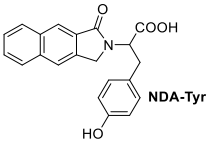 NDA-Tyr	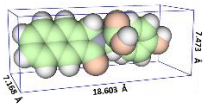	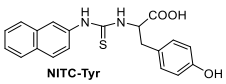 NITC-Tyr	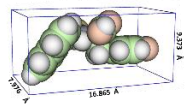
Charged	Glu	E	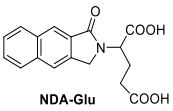 NDA-Glu	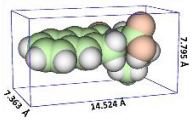	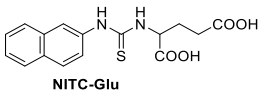 NITC-Glu	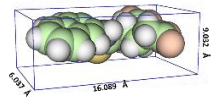
	His	H	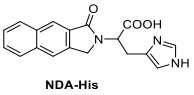 NDA-His	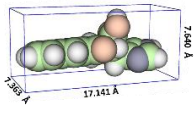	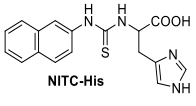 NITC-His	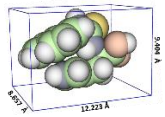
	Asp	D	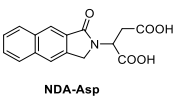 NDA-Asp	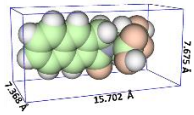	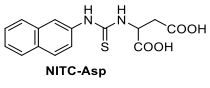 NITC-Asp	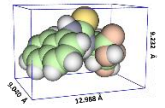

Table S2 The molecular volume calculated according to the space-filling structures, mean I/I_0 and dwell time, together with the corresponding standard derivation (S.D.) of selected amino acids derivatized with NDA and NITC, respectively.

			Volume ($Å^3$)	I/I_0	S.D.	Dwell time	S.D.
NDA	GLy	G	559.007	0.053	0.005	1.138	0.625
	Ala	A	664.277	0.163	0.076	0.604	0.219
	Val	V	833.599	0.078	0.031	0.321	0.141
	Glu	E	833.599	0.154	0.077	0.154	0.125
	Ser	S	866.570	0.192	0.018	0.307	0.188
	Asp	D	888.645	0.267	0.063	0.556	0.333
	His	H	963.789	0.084	0.037	0.185	0.068
	Phe	F	974.437	0.226	0.051	1.193	0.439
	Tyr	Y	996.214	0.099	0.029	0.295	0.179
NITC	GLy	G	734.665	0.065	0.019	0.126	0.032
	Ala	A	830.239	0.132	0.085	0.269	0.154
	Val	V	857.548	0.217	0.036	0.218	0.036
	Glu	E	877.271	0.249	0.132	1.175	0.346
	Ser	S	942.151	0.289	0.035	0.234	0.160
	His	H_1	994.757	0.347	0.096	0.625	0.634
	His	H_2	994.757	0.492	0.201	0.625	0.634
	Asp	D	1083.875	0.134	0.019	0.209	0.159
	Phe	F	1194.366	0.178	0.055	0.130	0.016
	Tyr	Y	1264.575	0.439	0.073	2.886	0.540

Spectral Data

2-(1-oxo-1,3-dihydro-2H-benzo[f]isoindol-2-yl)acetic acid

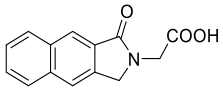

NDA-Gly

^{1}H NMR (DMSO-d_6, 400 MHz): δ 8.34 (s, 1 H), 8.17-8.02 (m, 3 H), 7.64 (m, 2 H), 4.67 (br, 2 H), 4.36 (br, 2 H). ^{13}C NMR (DMSO-d_6, 100 MHz): δ 170.9, 167.9, 137.3, 135.2, 132.8, 130.4, 129.8, 128.5, 128.1, 126.7, 123.5, 122.4, 50.4, 44.1. HRMS: $[M + H]^+$ *m/z* calcd for $C_{14}H_{11}NO_3H^+$, 242.0812; found, 242.0812.

2-(1-Oxo-1,3-dihydro-2H-benzo[f]isoindol-2-yl)propanoic acid

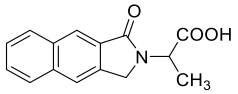

NDA-Ala

^{1}H NMR (DMSO-d_6, 400 MHz): δ 8.36 (s, 1 H), 8.16 (d, 1 H, *J*=7.9 Hz), 8.11 (s, 1 H), 8.05 (d, 1 H, *J*=8.1 Hz), 7.73-7.56 (m, 2 H), 4.92 (q, 1 H, *J*=7.5 Hz), 4.66 (dd, 2 H, J_1=17.3 Hz, J_2=4.3 Hz), 1.55 (d, 3 H, *J*=7.5 Hz). ^{13}C NMR (DMSO-d_6, 100 MHz): δ 173.0, 167.4, 136.9, 134.8, 132.4, 130.3, 129.4, 128.1, 127.8, 126.3, 123.1, 122.1, 49.4, 46.6, 15.3. HRMS: $[M - H]^-$ *m/z* calcd for $C_{15}H_{12}NO_3^-$, 254.0823; found, 254.0823.

3-methyl-2-(1-oxo-1,3-dihydro-2H-benzo[f]isoindol-2-yl)butanoic acid

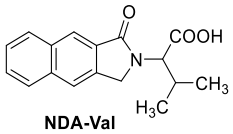

NDA-Val

^{1}H NMR (DMSO-d_6, 400 MHz): δ 13.04 (s, 1 H), 8.38 (s, 1 H), 8.16 (d, *J*=8.1 Hz, 1 H), 8.13 (s, 1 H), 8.05 (d, *J*=8.2 Hz, 1 H), 7.67-7.58 (m, 2 H), 4.80-4.67 (m, 2 H), 4.60 (d, *J*=9.8 Hz, 1 H), 2.39-2.30 (m,

1 H), 1.06 (d, *J*=6.6 Hz, 3 H), 0.88 (d, *J*=6.3 Hz, 3 H). ^{13}C NMR (DMSO-d_6, 100 MHz): δ 172.2, 168.1, 137.3, 135.2, 132.8, 130.1, 129.9, 128.5, 128.2, 126.7, 123.7, 122.5, 60.4, 47.4, 28.5,19.9, 19.6. HRMS: $[M + H]^+$ *m/z* calcd for $C_{17}H_{17}N_1O_3H^+$, 281.1281; found, 281.1281.

3-hydroxy-2-(1-oxo-1,3-dihydro-2H-benzo[f]isoindol-2-yl)propanoic acid

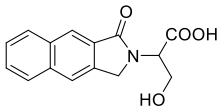

NDA-Ser

^{1}H NMR (DMSO-d_6, 400 MHz): δ 8.35 (s, 1 H), 8.15-8.12 (m, 2 H), 8.04 (d, *J*=8.2 Hz, 1 H), 7.66-7,57 (m, 2 H), 4.94-4.91 (m, 1 H), 4.74 (s, 1 H), 4.06-3.94 (m, 2 H). ^{13}C NMR (DMSO-d_6, 100 MHz): δ 171.2, 168.6, 137.6, 135.2, 132.7, 130.4, 129.8, 128.5, 128.3, 126.8, 123.4, 122.4, 60.0, 57.0, 48.1. HRMS: $[M + H]^+$ *m/z* calcd for $C_{15}H_{13}NO_4H^+$, 274.0917; found, 274.0917.

2-(1-Oxo-1,3-dihydro-2H-benzo[f]isoindol-2-yl)-3-phenylpropanoic acid

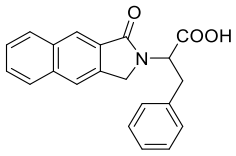

NDA-Phe

^{1}H NMR (DMSO-d$_6$, 400 MHz): δ 13.2 (s, 1 H), 8.27 (s, 1 H), 8.11 (d, 1 H, *J*=8.1 Hz), 8.05 (s, 1 H), 8.01 (d, 1 H, *J*=8.1 Hz), 7.64-7.55 (m, 2 H), 7.28 (d, 2 H, *J*=7.2 Hz), 7.21 (t, 2 H, *J*=7.5 Hz), 7.12 (t, 1 H, *J*=7.2 Hz), 5.21 (q, 1 H, *J*=5.4 Hz), 4.60 (q, 2 H, *J*=14.6 Hz), 3.45-3.16 (m, 2 H). ^{13}C NMR (DMSO-d$_6$, 100 MHz): δ 172.3, 167.9, 137.9, 137.0, 135.1, 132.7, 130.2, 129.8, 129.0, 128.8, 128.4, 128.1, 126.9, 126.7, 123.6, 122.5, 55.5, 47.8, 35.0. HRMS: $[M + H]^+$ *m/z* calcd for $C_{21}H_{17}NO_3H^+$, 332.1281; found, 332.1279.

3-(4-Hydroxyphenyl)-2-(1-oxo-1,3-dihydro-2H-benzo[f]isoindol-2-yl)propanoic acid

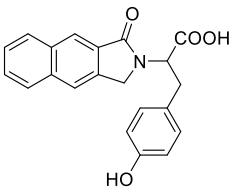

NDA-Tyr

^{1}H NMR (DMSO-d_6, 400 MHz): δ 9.46 (s, 1 H), 8.23 (s, 1 H), 8.06 (d, 1 H, *J*=8.2 Hz), 8.02 (s, 1 H), 8.00 (d, 1 H, *J*=8.1 Hz), 7.63-7.53 (m, 2 H), 7.05 (d, 2 H, *J*=8.4 Hz), 6.58 (d, 2 H, *J*=8.4 Hz), 5.11 (q, 1 H, *J*=5.4 Hz), 4.56 (dd, 2 H, J_1=17.2 Hz, J_2=3.8 Hz), 3.30/3.10 (q, 2 H, J_1=6.4 Hz, J_2=8.7 Hz). ^{13}C NMR (DMSO-d_6, 100 MHz): δ 171.9, 167.4, 155.8, 136.6, 134.6, 132.3, 129.9, 129.5, 129.3, 127.9, 127.8, 127.3, 126.2, 123.0, 121.9, 115.2, 55.2, 50.0, 33.8. HRMS: $[M - H]^-$ *m/z* calcd for $C_{21}H_{16}NO_4^-$, 346.1085; found, 346.1083.

2-(1-oxo-1,3-dihydro-2H-benzo[f]isoindol-2-yl)pentanedioic acid

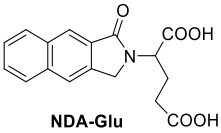

NDA-Glu

^{1}H NMR (DMSO-d_6, 400 MHz): δ 12.65 (s, 2 H), 8.37 (s, 1 H), 8.16 (d, *J*=8.0 Hz, 1 H), 8.10 (s, 1 H), 8.05 (d, *J*=8.1 Hz, 1 H), 7.72-7.51 (m, 2 H), 4.93-4.90 (m, 1 H), 4.68-4.59 (m, 2 H), 2.35-2.25 (m, 2 H), 3.35-2.08 (m, 2 H). ^{13}C NMR (DMSO-d_6, 100 MHz): δ 174.1, 172.5, 168.4, 137.4, 135.2, 132.8, 130.4, 129.8, 128.4, 128.2, 126.7, 123.6, 122.5, 53.7, 47.0, 30.8, 24.6. HRMS: $[M + H]^+$ *m/z* calcd for $C_{17}H_{15}NO_5H^+$, 314.1023; found, 314.1023.

3-(1H-imidazol-4-yl)-2-(1-oxo-1,3-dihydro-2H-benzo[f]isoindol-2-yl)propanoic acid

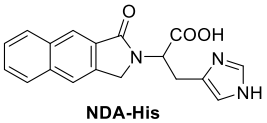

NDA-His

^{1}H NMR (DMSO-d$_6$, 400 MHz): δ 14.33 (s, 1 H), 8.99 (s, 1 H), 8.31 (s, 1 H), 8.13 (d, 1 H, *J*=8.2 Hz), 8.11 (s, 1 H), 8.04 (d, 1 H, *J*=8.2 Hz), 7.66-7.57 (m, 2 H), 7.42 (s, 1 H), 5.32 (q, 1 H, *J*=5.2 Hz), 4.81/4.81 (d, 2 H, *J*=16.6 Hz), 3.50-3.40 (m, 2 H). ^{13}C NMR (DMSO-d$_6$, 100 MHz): δ 170.7, 167.7, 136.6, 134.8, 133.8, 132.3, 129.5, 129.4, 129.3, 128.0, 127.9, 126.3, 123.3, 122.2, 116.8, 53.5, 46.9, 24.3. HRMS: [M - H]$^-$ *m/z* calcd for $C_{18}H_{15}N_3O_3^-$, 320.1041; found, 320.1038.

2-(1-Oxo-1,3-dihydro-2H-benzo[f]isoindol-2-yl)succinic acid

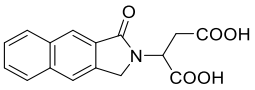

NDA-Asp

^{1}H NMR (DMSO-d$_6$, 400 MHz): δ 12.51 (s, 1 H), 8.36 (s, 1 H), 8.14 (d, 1 H, *J*=8.0 Hz), 8.10 (s, 1 H), 8.03 (d, 1 H, *J*=8.1 Hz), 7.65-7.56 (m, 2 H), 5.16 (q, 1 H, *J*=4.7 Hz), 4.60 (dd, 2 H, J_1=17.1 Hz, J_2=1.6 Hz), 3.04/2.93 (q, 2 H, *J*=7.6 Hz, *J*=8.6 Hz). ^{13}C NMR (DMSO-d$_6$, 100 MHz): δ 171.8, 171.3, 167.3, 136.8, 134.8, 132.4, 129.9, 129.4, 128.0, 127.8, 126.3, 123.2, 122.1, 51.2, 47.7, 34.5. HRMS: [M - H]$^-$ *m/z* calcd for $C_{16}H_{12}NO_5^-$, 298.0721; found, 298.0717.

(Naphthalen-2-ylcarbamothioyl)glycine

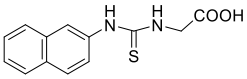

NITC-Gly

^{1}H NMR (DMSO-*d$_6$*, 400 MHz): δ 12.71 (s, 1 H), 10.11 (s, 1 H), 8.05-8.02 (m, 2 H), 7.89-7.83 (m, 3 H), 7.56 (q, *J*=3.6 Hz, 1 H), 7.52-7.43 (m, 2 H), 4.25 (d, *J*=5.4 Hz, 2 H). ^{13}C NMR (DMSO-*d$_6$*, 100 MHz): δ 180.6, 170.6, 136.2, 132.7, 129.9, 127.7, 127.0, 126.9, 125.9, 124.7, 122.9, 119.0, 45.2. HRMS: [M + H]$^+$ *m/z* calcd for $C_{13}H_{12}N_2O_2SH^+$, 261.0692; found, 261.0692.

(Naphthalen-2-ylcarbamothioyl)alanine

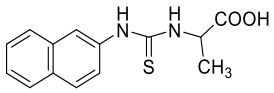

NITC-Ala

^{1}H NMR (DMSO-d$_6$, 400 MHz): δ 10.62 (s, 1 H), 8.03-8.00 (m, 3 H), 7.89 (d, 1 H, *J*=1.7 Hz), 7.64-7.57 (m, 2 H), 7.43 (q, 1 H, *J*=3.6 Hz), 4.57-4.50 (m, 1 H), 1.45 (d, 3 H, *J*=7.1 Hz,). ^{13}C NMR (DMSO-d$_6$, 100 MHz): δ 182.6, 175.6, 133.1, 133.0, 131.4, 128.7, 128.4, 128.2, 128.1, 127.4, 127.1, 127.0, 55.7, 16.7. HRMS: [M + H]$^+$ *m/z* calcd for $C_{14}H_{14}N_2O_2SH^+$, 275.0849; found, 275.0849.

(Naphthalen-2-ylcarbamothioyl)valine

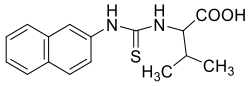

NITC-Val

^{1}H NMR (DMSO-*d*$_6$, 400 MHz): δ 10.69 (s, 1 H), 8.03-8.01 (m, 3 H), 7.84 (s, 1 H), 7.63-7.57 (m, 2 H), 7.36 (d, *J*=8.6 Hz, 1 H), 4.41 (d, *J*=3.3 Hz, 1 H), 2.26-2.22 (m, 1 H), 1.09 (d, *J*=6.8 Hz, 3 H), 0.97 (d, *J*=6.7 Hz, 3 H). ^{13}C NMR (DMSO-*d*$_6$, 100 MHz): δ 183.4, 174.5, 133.2, 133.0, 131.3, 128.9, 128.5, 128.1, 128.0, 127.5, 127.1, 126.9, 65.1, 31.0, 18.8, 16.7. HRMS: [M + H]$^+$ *m/z* calcd for $C_{16}H_{18}N_2O_2SH^+$, 303.1162; found, 303.1162.

(Naphthalen-2-ylcarbamothioyl)serine

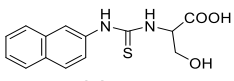

NITC-Ser

^{1}H NMR (DMSO-d$_6$, 400 MHz): δ 10.54 (s, 1 H), 8.03-8.00 (m, 3 H), 7.82 (d, *J*=2.0 Hz, 1 H), 7.63-7.57 (m, 2 H), 7.36 (q, *J*=3.6 Hz, 1 H), 5.40-5.37 (m, 1 H), 4.52-4.50 (m, 1 H), 3.90-3.76 (m, 2 H). ^{13}C NMR (DMSO-d$_6$, 100 MHz): δ 183.5, 173.7, 133.1, 132.9, 131.5, 128.7, 128.4, 128.1, 128.06, 127.4, 127.1, 127.0, 62.8, 60.2. HRMS: [M + H]$^+$ *m/z* calcd for $C_{14}H_{14}N_2O_3SH^+$, 291.0798; found, 291.0798.

(Naphthalen-2-ylcarbamothioyl)phenylalanine

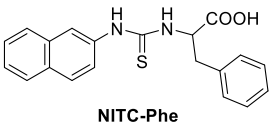

NITC-Phe

^{1}H NMR (DMSO-d$_6$, 400 MHz): δ 10.68 (s, 1 H), 7.96-7.86 (m, 3 H), 7.61-7.53 (m, 2 H), 7.38-7.32 (m, 4 H), 7.26-7.23 (m, 2 H), 6.85 (dd, 1 H, J_1=10.6 Hz, J_2= 6.8 Hz), 4.83 (t, 1 H, J=4.3 Hz), 3.16 (d, 2 H, J=4.5 Hz). ^{13}C NMR (DMSO-d$_6$, 100 MHz): δ 182.8, 174.1, 135.0, 133.0, 132.9, 131.1, 130.0, 128.69, 128.67, 128.3, 128.1, 127.8, 127.6, 127.4, 127.1, 126.5, 60.8, 36.7. HRMS: [M - H]$^-$ *m/z* calcd for $C_{20}H_{17}N_2O_2S^-$, 349.1016; found, 349.1011.

(Naphthalen-2-ylcarbamothioyl)tyrosine

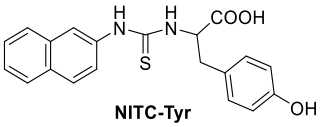

NITC-Tyr

^{1}H NMR (DMSO-d$_6$, 400 MHz): δ 10.06 (s, 1 H), 9.62 (s, 1 H), 7.94-7.88 (m, 2 H), 7.84 (d, 1 H, J=7.0 Hz), 7.57-7.55 (m, 2 H), 7.25 (s, 1H), 7.02 (d, 2 H, J=7.3 Hz), 6.86 (d, 1 H, J=8.6 Hz), 6.73 (d, 2 H, J=7.1 Hz), 4.70 (s, 1 H), 3.05 (d, J=2.5 Hz, 2 H). ^{13}C NMR (DMSO-d$_6$, 100 MHz): δ 182.8, 174.4, 156.9, 132.89, 132.87, 131.4, 131.1, 128.8, 128.2, 128.1, 127.8, 127.6, 127.2, 126.5, 124.8, 115.4, 61.1, 35.8. HRMS: [M - H]$^-$ *m/z* calcd for $C_{20}H_{18}N_2O_3S^-$, 365.0965; found, 365.0965.

(Naphthalen-2-ylcarbamothioyl)glutamic acid

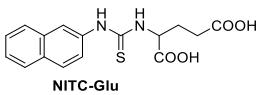

NITC-Glu

^{1}H NMR (DMSO-*d$_6$*, 400 MHz): δ 12.33 (s, 1 H), 10.68 (s, 1 H), 8.02-7.96 (m, 3 H), 7.89 (d, J=1.7 Hz, 1 H), 7.63-7.57 (m, 2 H), 7.43 (q, J=3.6 Hz, 1 H), 4.53 (t, J=6.4 Hz, 1 H), 3.35 (br, 2 H), 2.17-1.96

(m, 2 H). ^{13}C NMR (DMSO-d_6, 100 MHz): δ 183.1, 174.7, 174.0, 133.1, 132.9, 131.4, 128.7, 128.4, 128.2, 128.1, 127.4, 127.1, 127.0, 59.1, 29.4, 26.8. HRMS: $[M + H]^+$ *m/z* calcd for $C_{16}H_{16}N_2O_4SH^+$, 333.0904; found, 333.0904.

(Naphthalen-2-ylcarbamothioyl)histidine

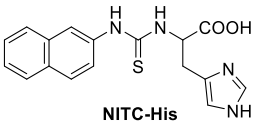

NITC-His

^{1}H NMR (DMSO-d_6, 400 MHz): δ 10.23 (s, 1 H), 8.29 (d, 1 H, *J*=8.7 Hz), 8.24 (s, 1 H), 8.00 (s, 1 H), 7.84 (d, 2 H, *J*=8.7 Hz), 7.80 (d, 1 H, *J*=8.0 Hz), 7.51-7.40 (m, 3 H), 5.18 (q, 1 H, *J*=5.0 Hz), 3.19-3.09 (m, 2 H). ^{13}C NMR (DMSO-d_6, 100 MHz): δ 180.5, 172.4, 136.7, 134.3, 133.2, 131.6, 130.0, 128.2, 127.5, 127.4, 126.4, 125.2, 123.2, 119.2, 116.5, 56.4, 27.8. HRMS: $[M - H]^-$ *m/z* calcd for $C_{17}H_{15}N_4O_2S^-$, 339.0921; found, 339.0917.

(Naphthalen-2-ylcarbamothioyl)aspartic acid

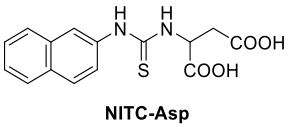

NITC-Asp

^{1}H NMR (DMSO-d_6, 400 MHz): δ 12.8 (s, 1 H), 10.41 (s, 1 H), 8.03-7.97 (m, 3 H), 7.83 (d, 1 H, *J*=1.8 Hz), 7.64-7.57 (m, 2 H), 7.40 (q, 1 H, *J*=3.5 Hz), 4.68 (q, 1 H, *J*=4.4 Hz), 3.00/2.84 (q, 2 H, *J*=7.3 Hz). ^{13}C NMR (DMSO-d_6, 100 MHz): δ 183.2, 174.2, 170.8, 132.7, 132.5, 131.3, 128.3, 128.0, 127.7, 127.6, 126.9, 126.6,126.4, 55.9, 34.8. HRMS: $[M + H]^+$ *m/z* calcd for $C_{15}H_{14}N_2O_4SH^+$, 319.0747; found, 319.0747.

NMR Data

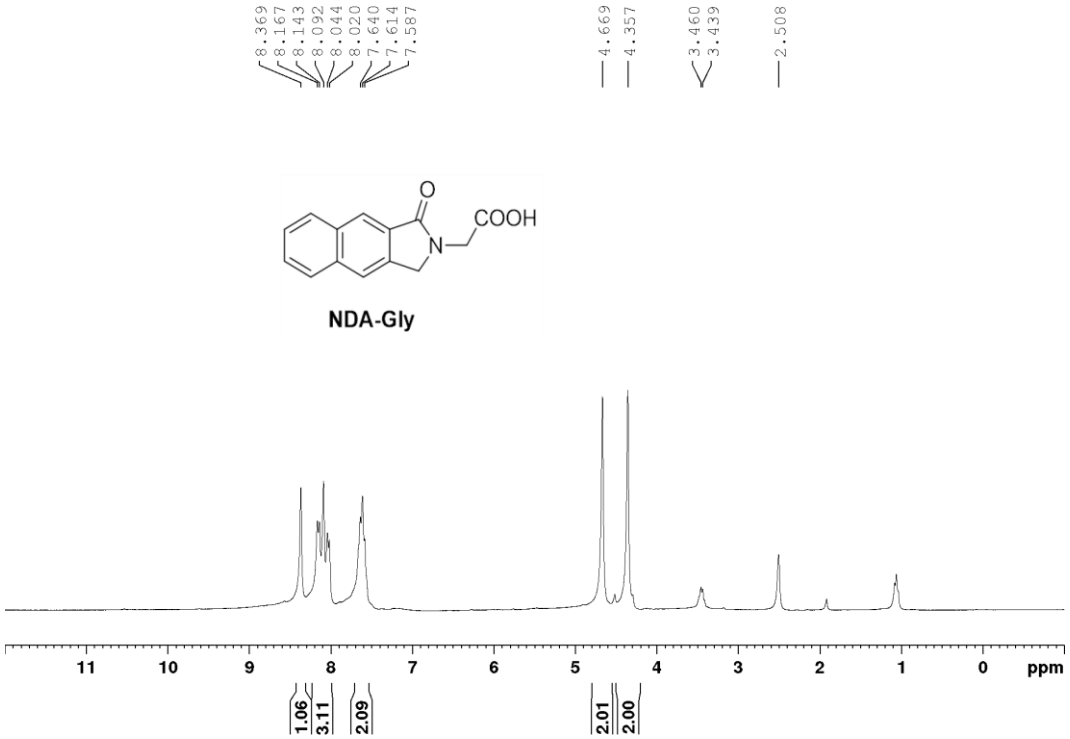

Fig. S4 ^{1}H NMR spectrum of NDA-Gly.

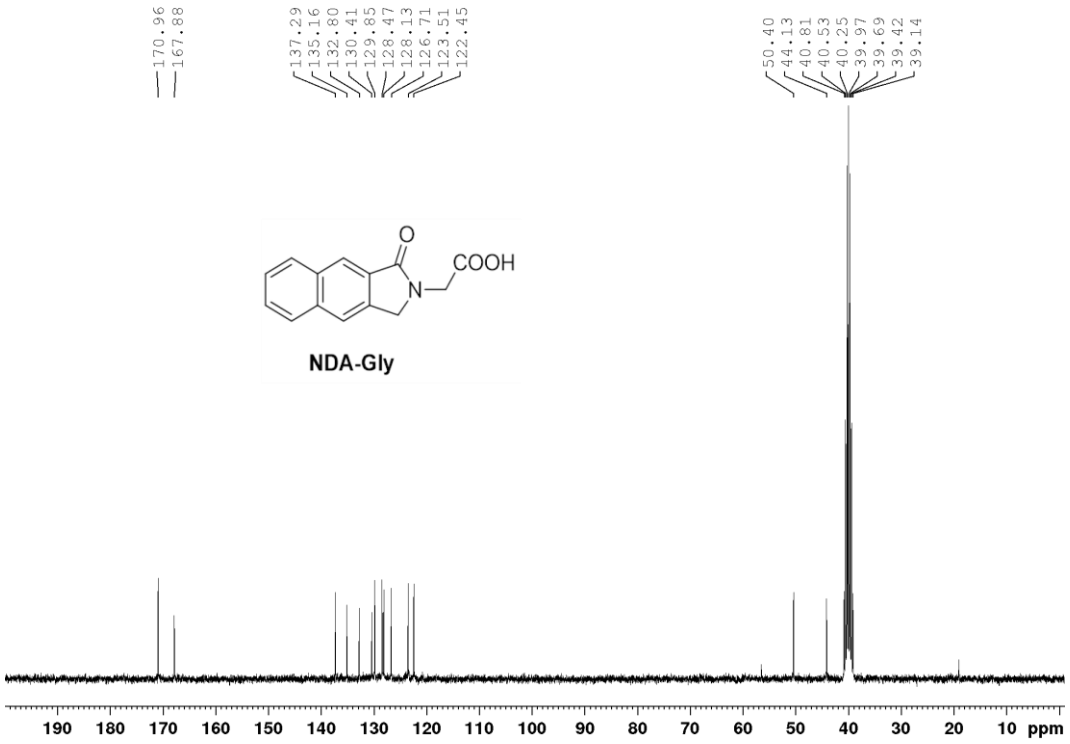

Fig. S5 ^{13}C NMR spectrum of NDA-Gly.

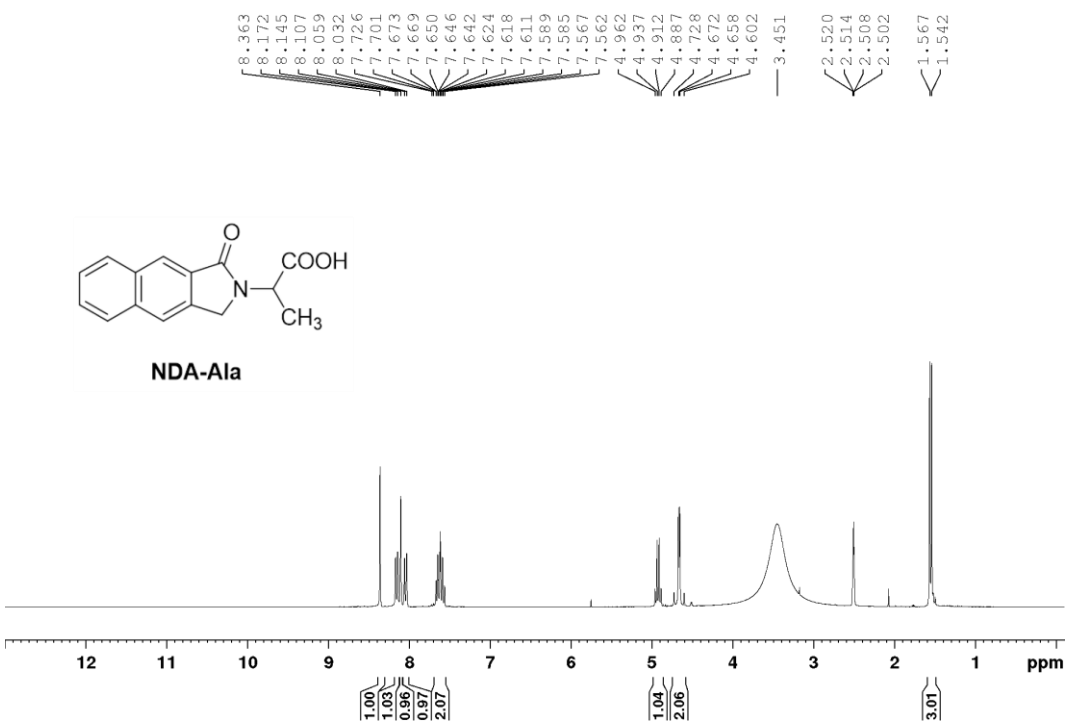

Fig. S6 ^{1}H NMR spectrum of NDA-Ala.

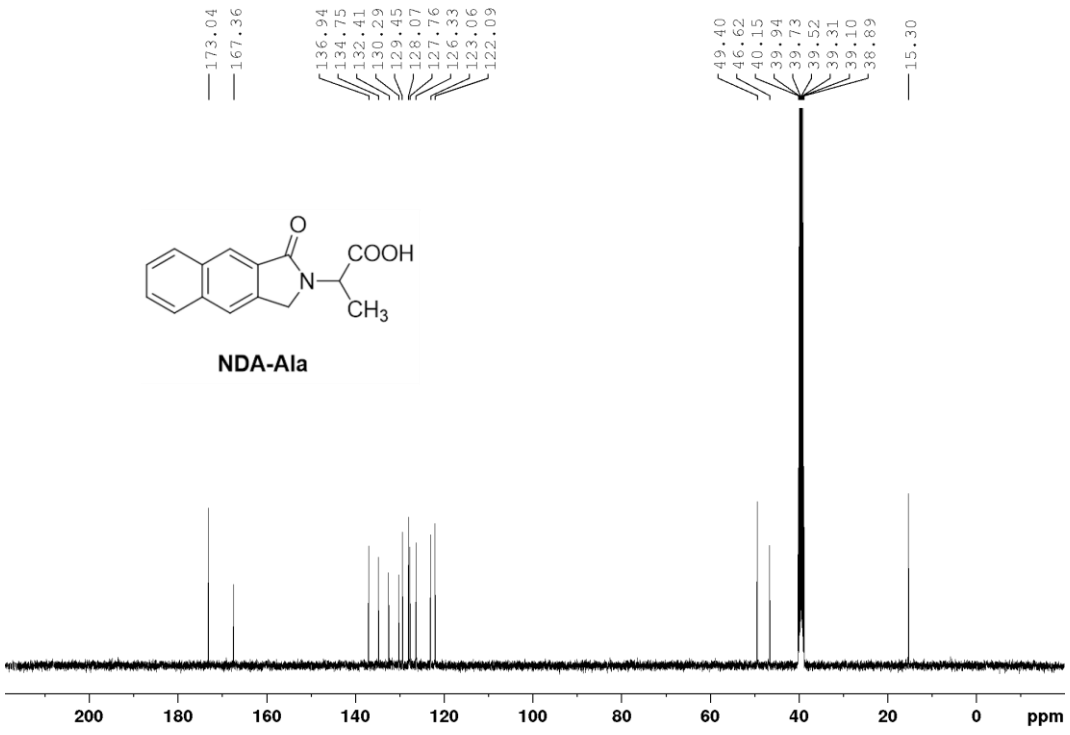

Fig. S7 ^{13}C NMR spectrum of NDA-Ala.

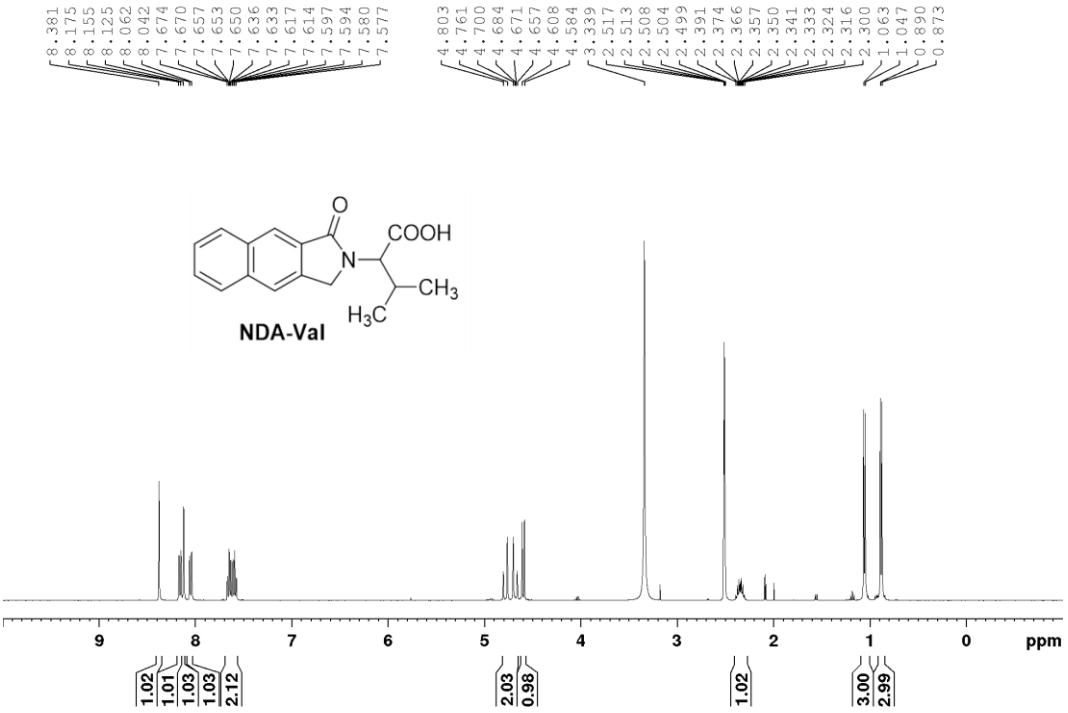

Fig. S8 ^{1}H NMR spectrum of NDA-Val.

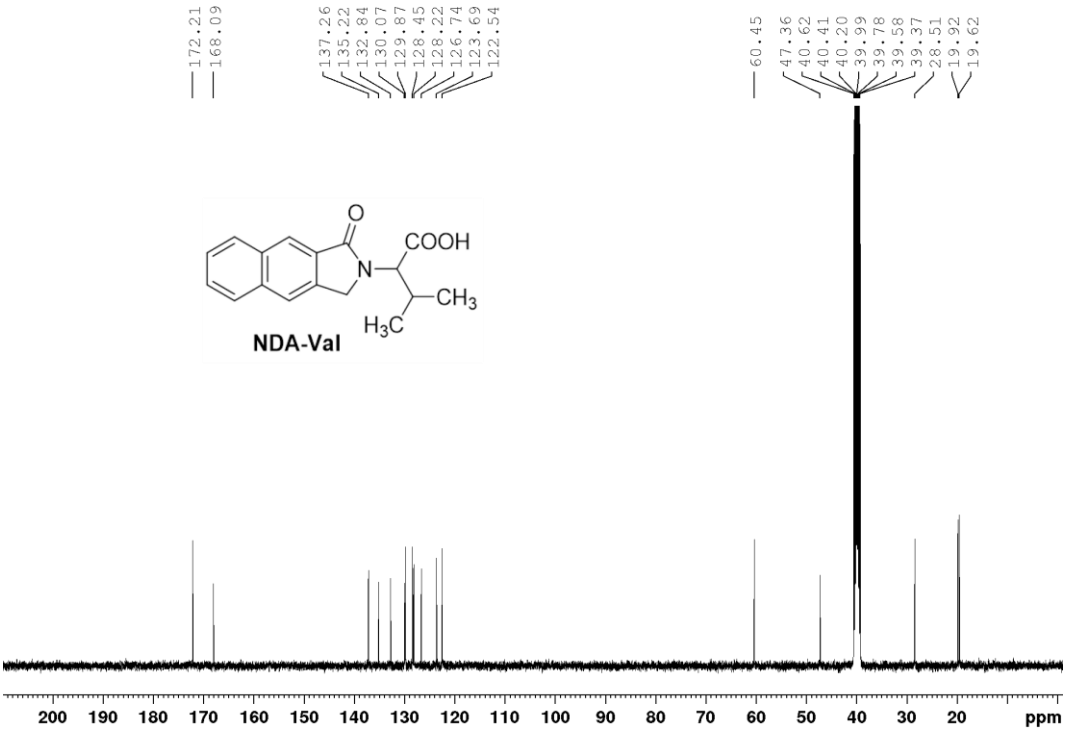

Fig. S9 ^{13}C NMR spectrum of NDA-Val.

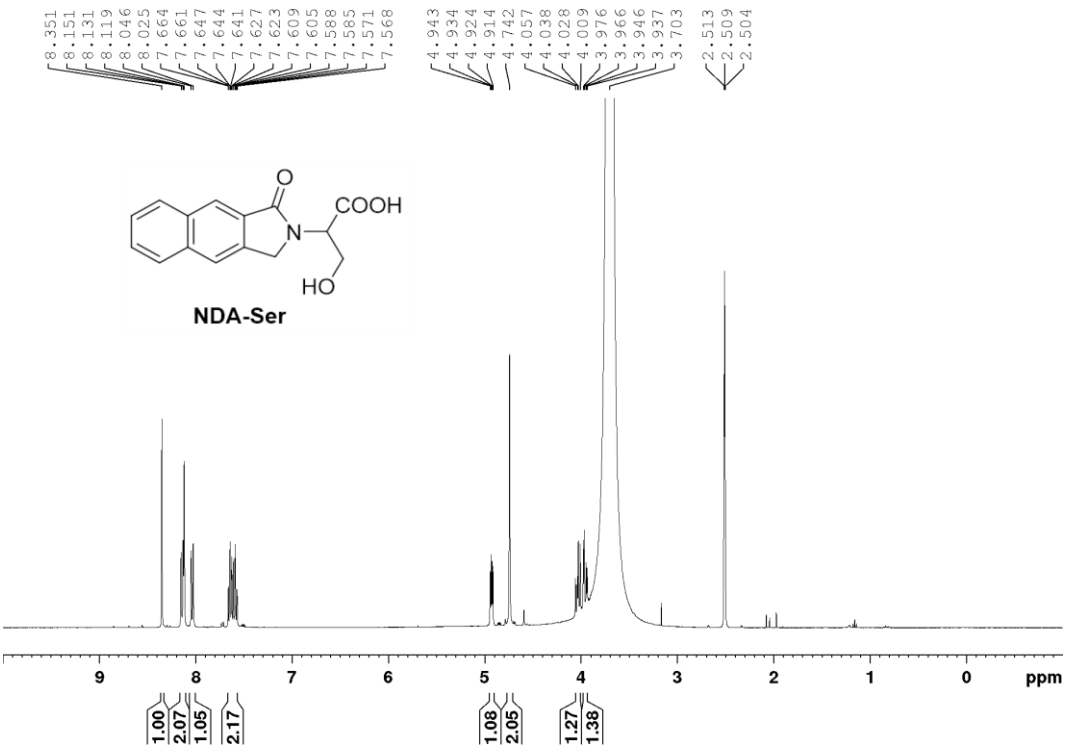

Fig. S10 ^{1}H NMR spectrum of NDA-Ser.

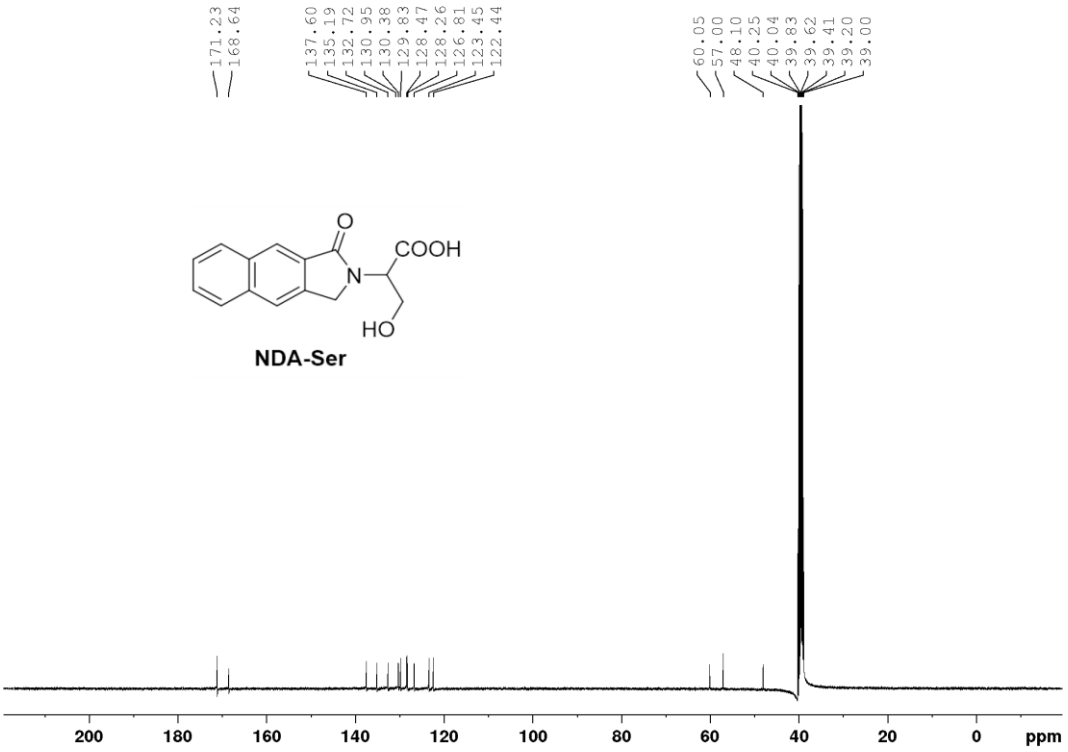

Fig. S11 ^{13}C NMR spectrum of NDA-Ser.

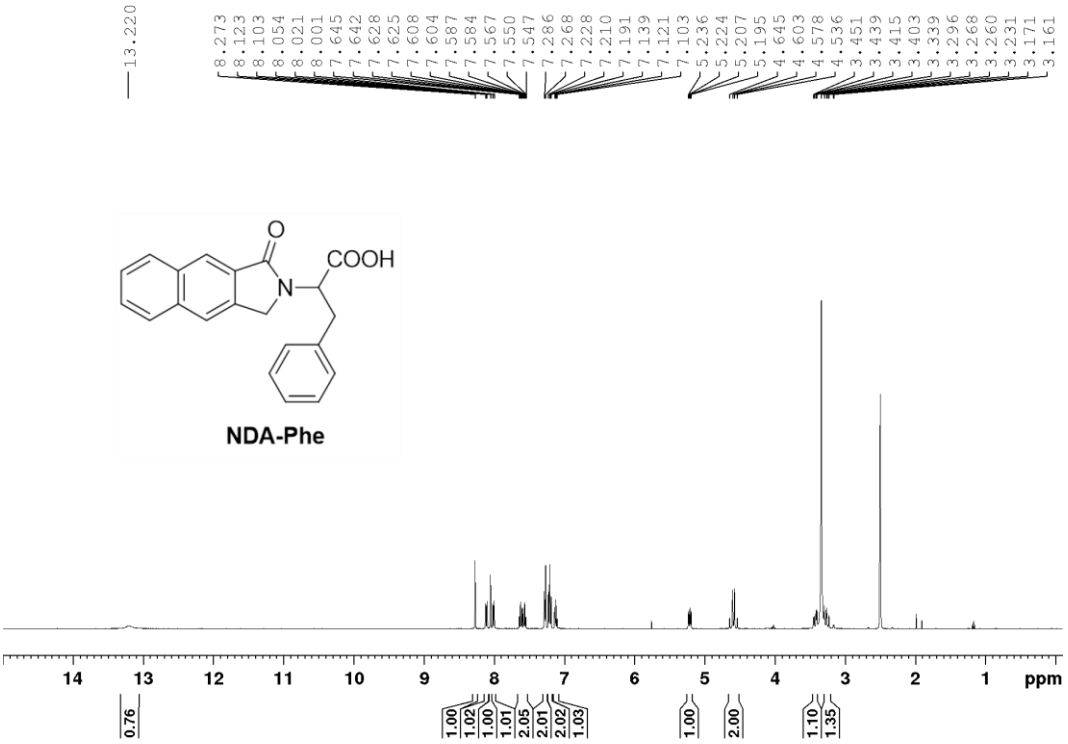

Fig. S12 ^{1}H NMR spectrum of NDA-Phe.

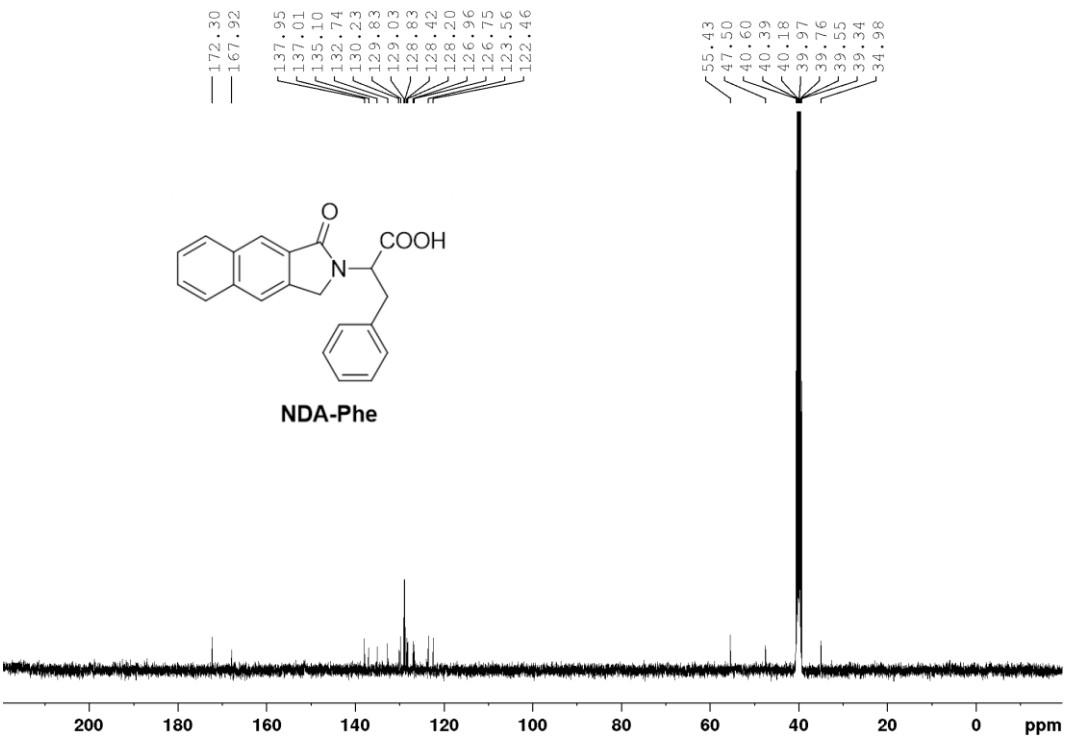

Fig. S13 ^{13}C NMR spectrum of NDA-Phe.

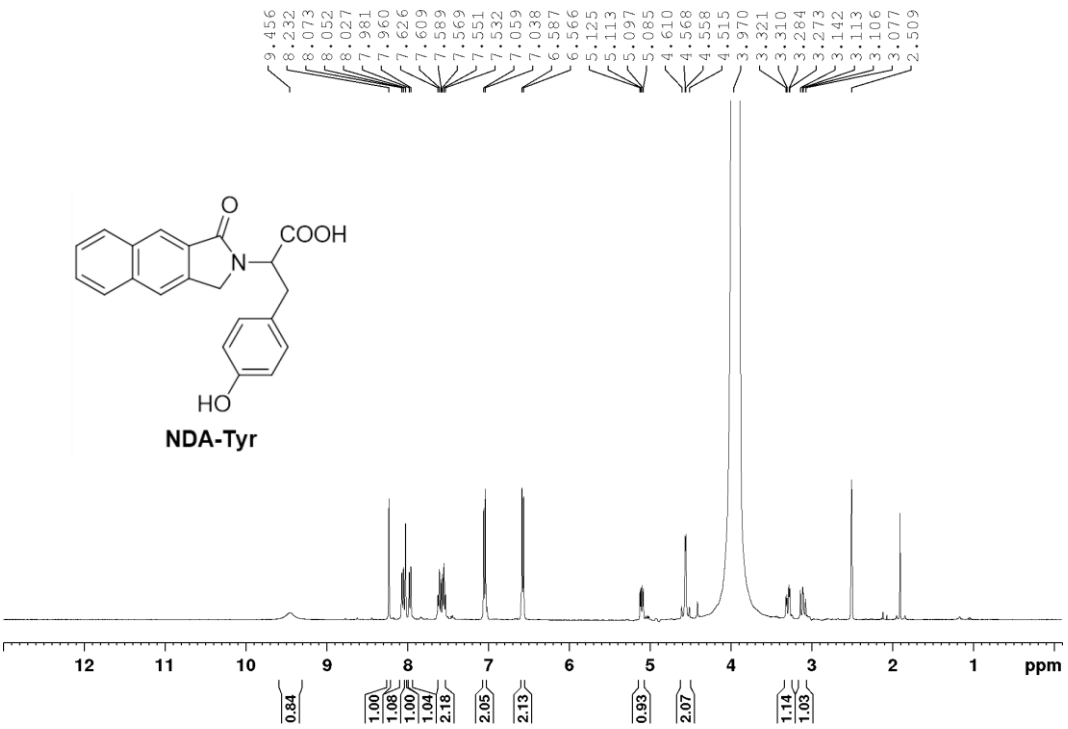

Fig. S14 ^{1}H NMR spectrum of NDA-Tyr.

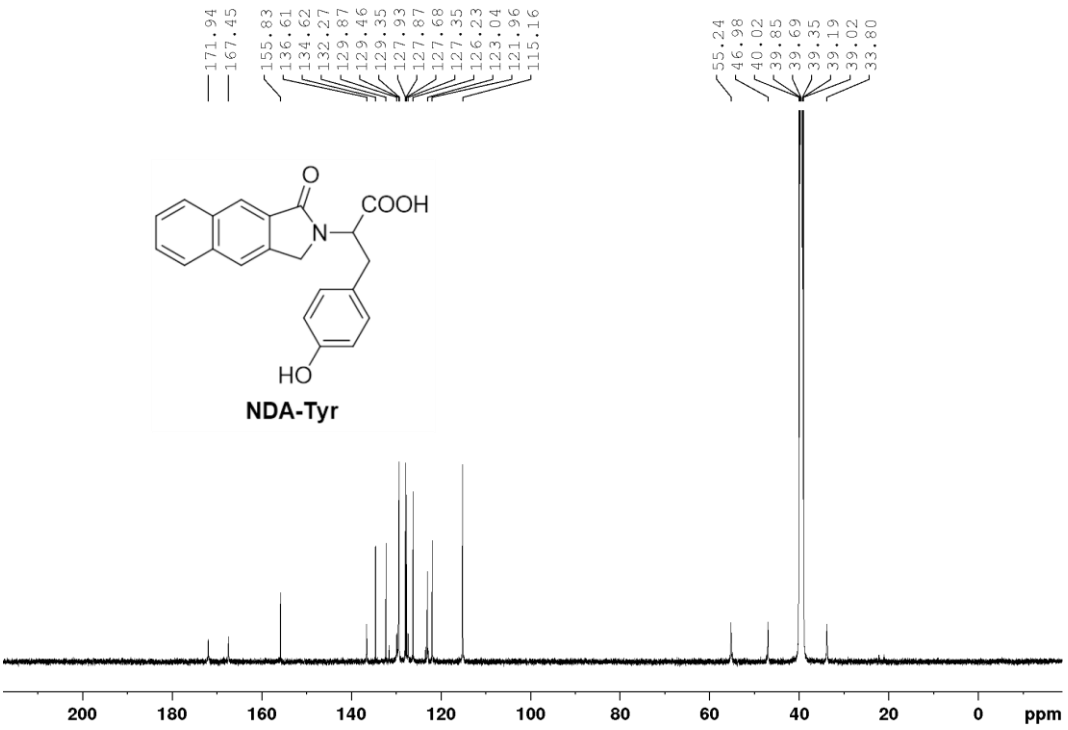

Fig. S15 ^{13}C NMR spectrum of NDA-Tyr.

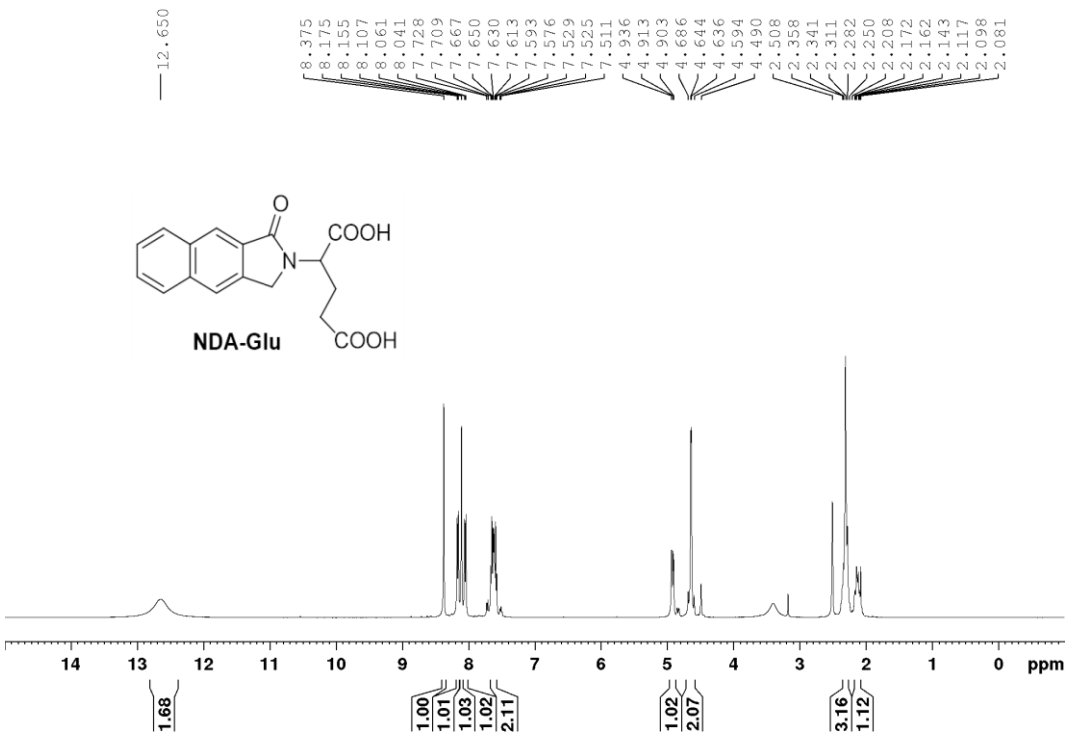

Fig. S16 ^{1}H NMR spectrum of NDA-Glu.

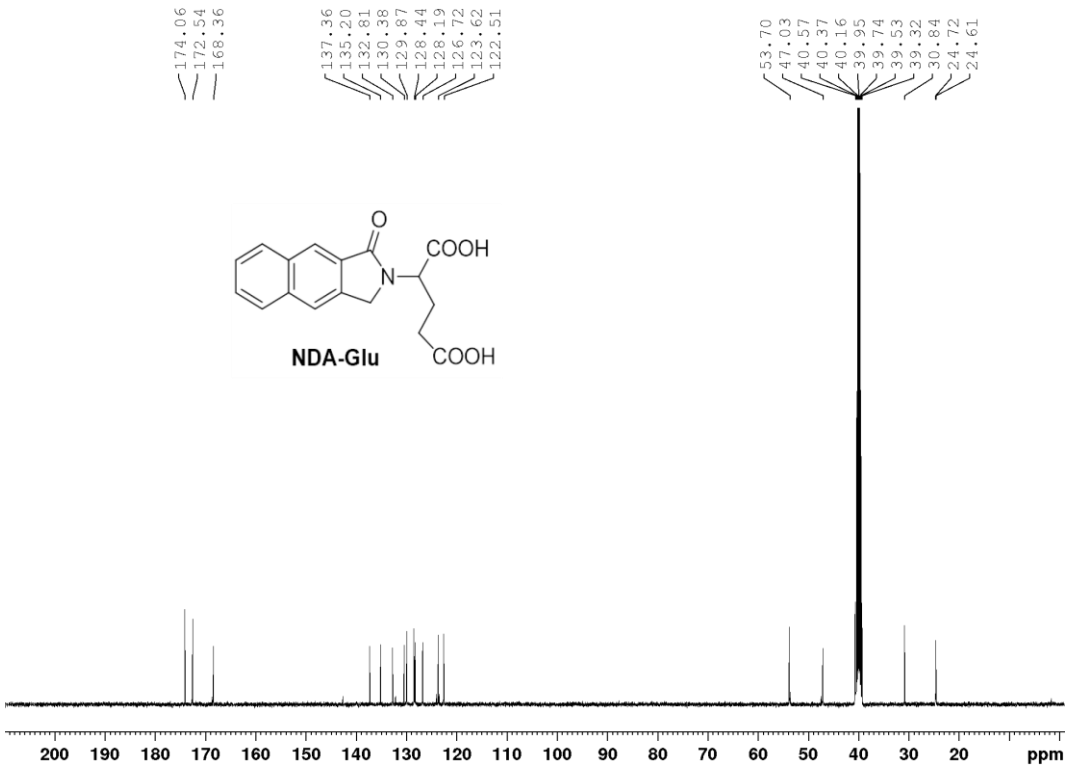

Fig. S17 ^{13}C NMR spectrum of NDA-Glu.

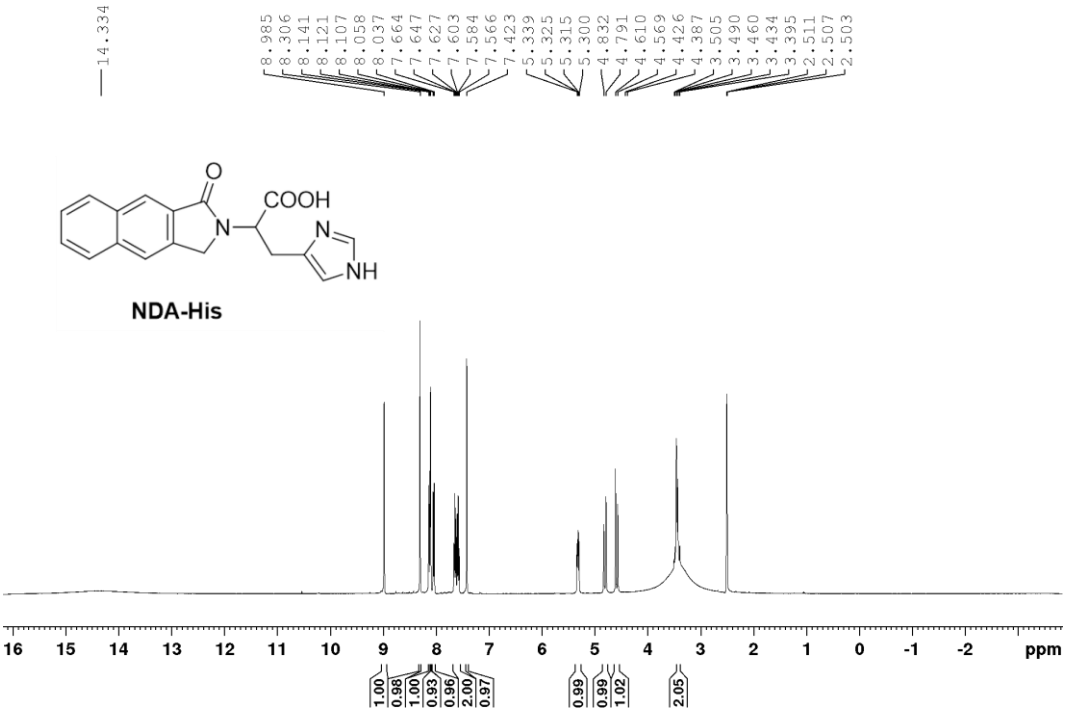

Fig. S18 ^{1}H NMR spectrum of NDA-His.

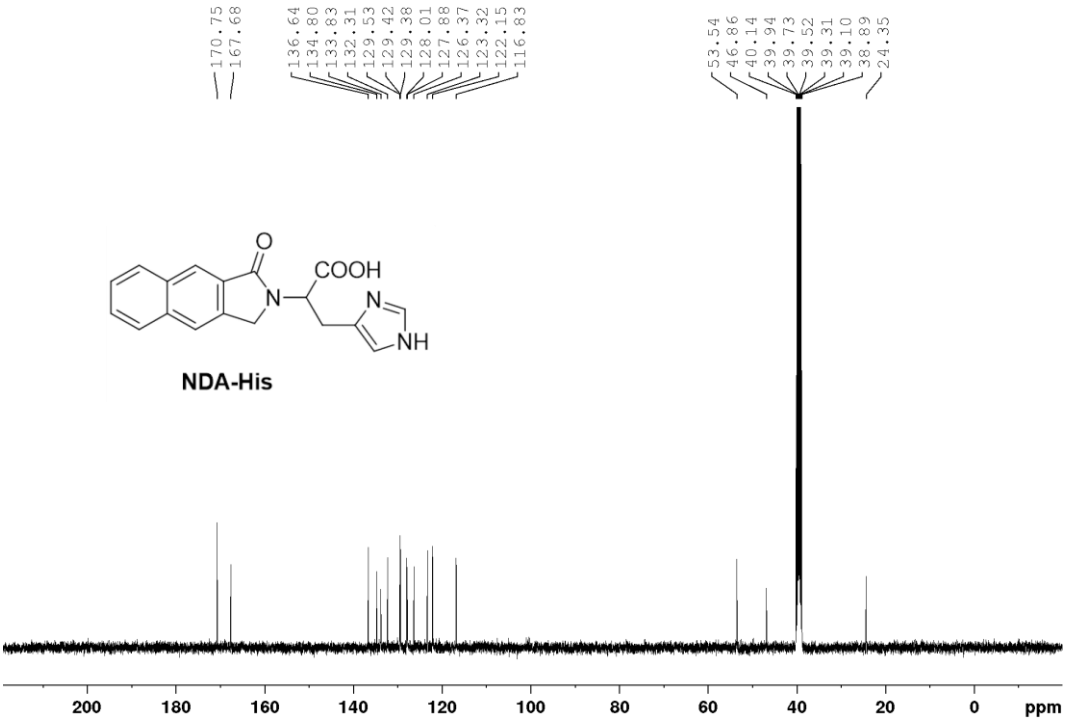

Fig. S19 ^{13}C NMR spectrum of NDA-His.

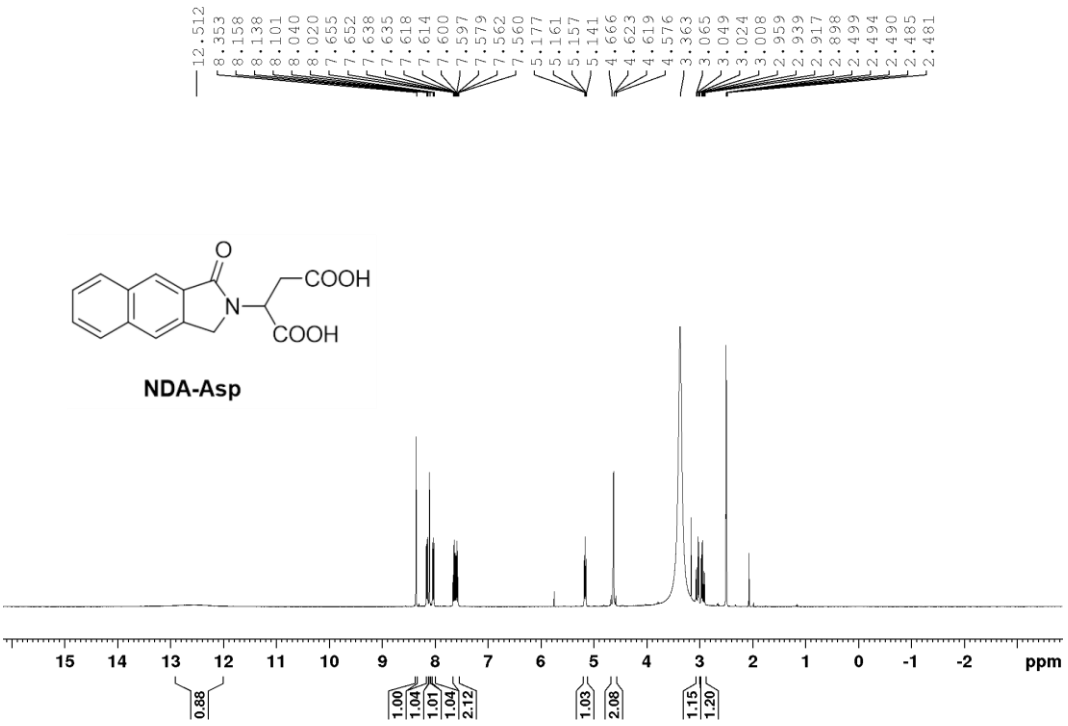

Fig. S20 ^{1}H NMR spectrum of NDA-Asp.

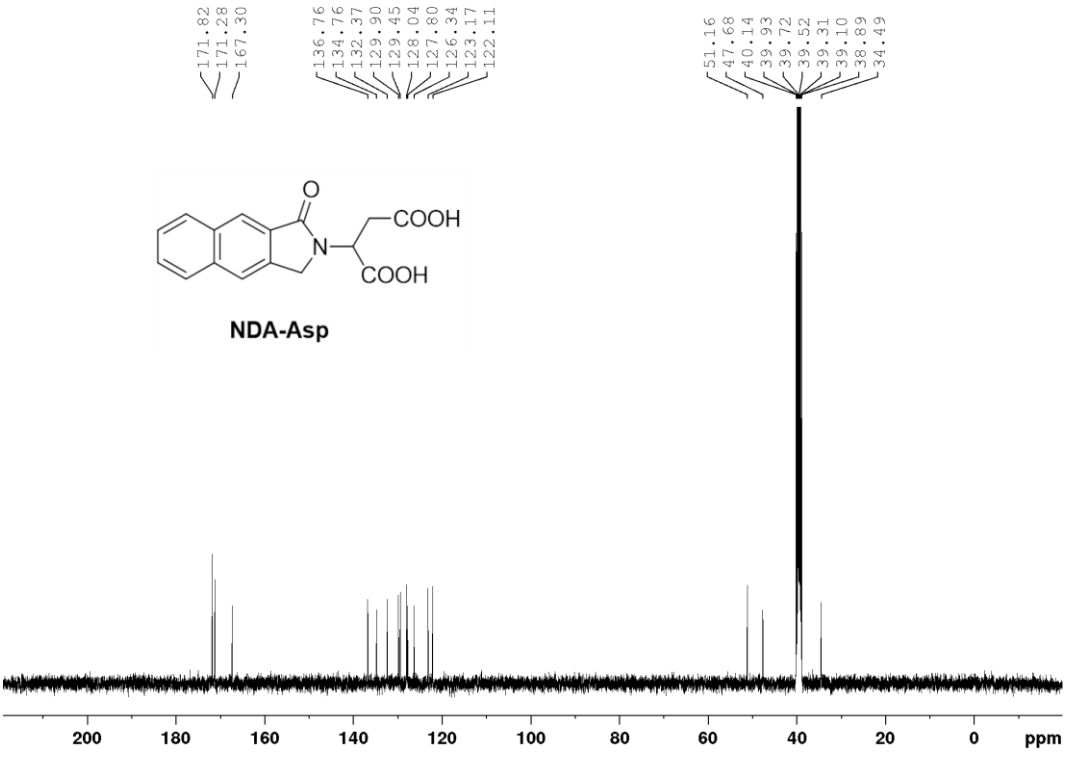

Fig. S21 ^{13}C NMR spectrum of NDA-Asp.

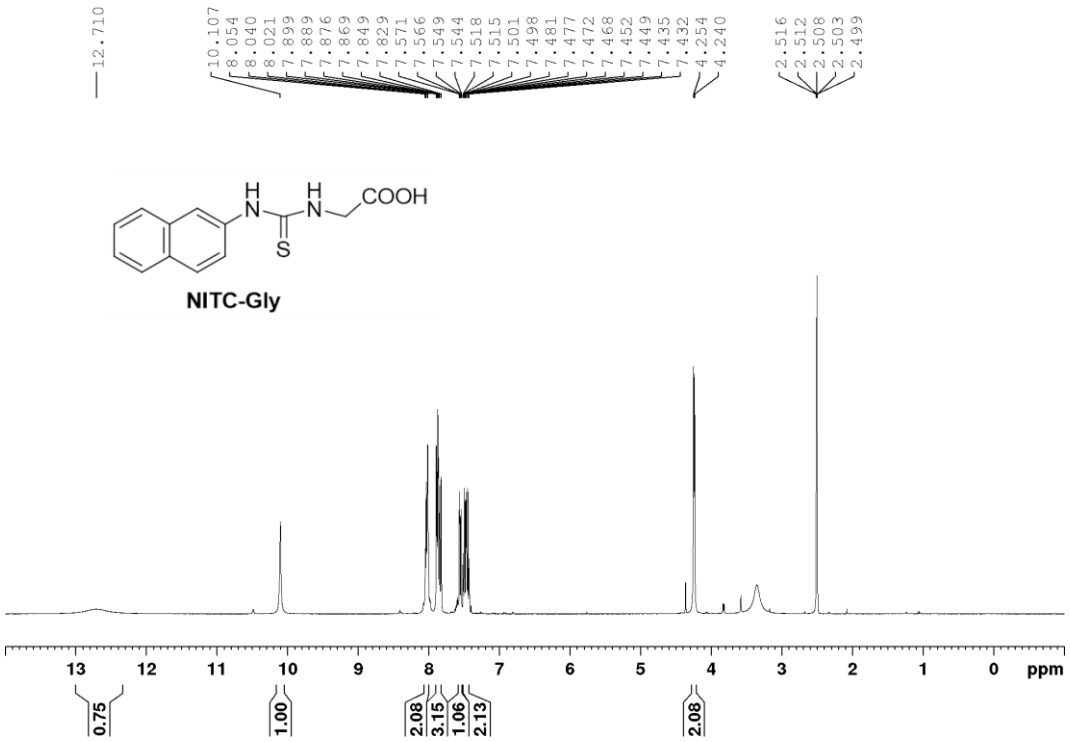

Fig. S22 ^{1}H NMR spectrum of NITC-Gly.

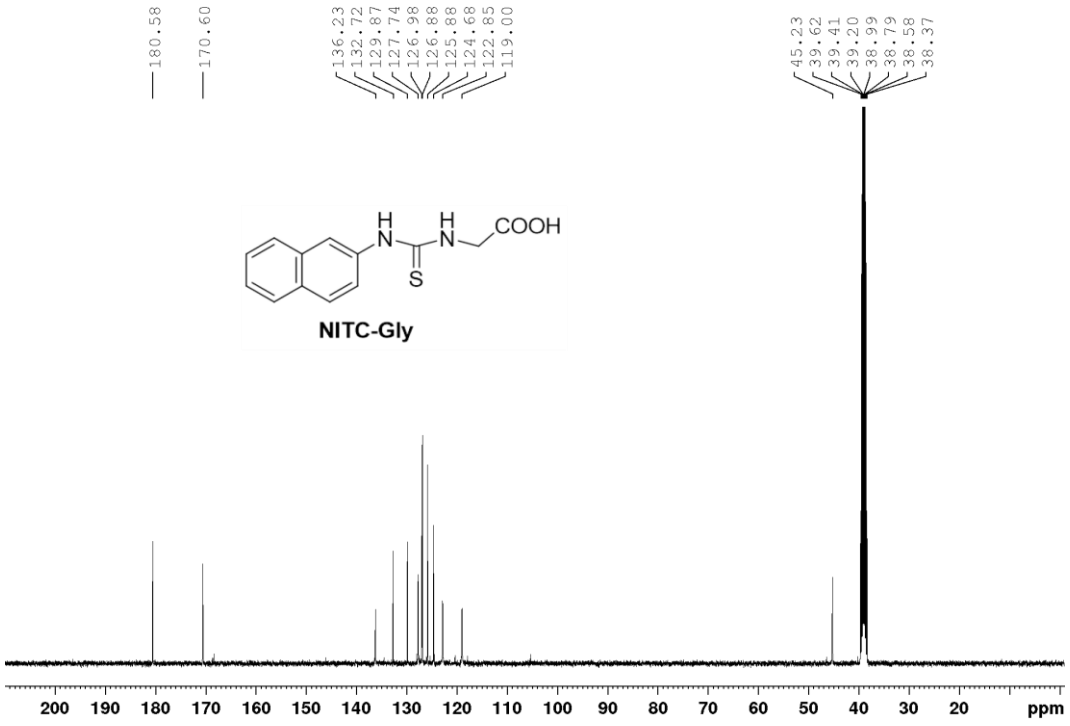

Fig. S23 ^{13}C NMR spectrum of NITC-Gly.

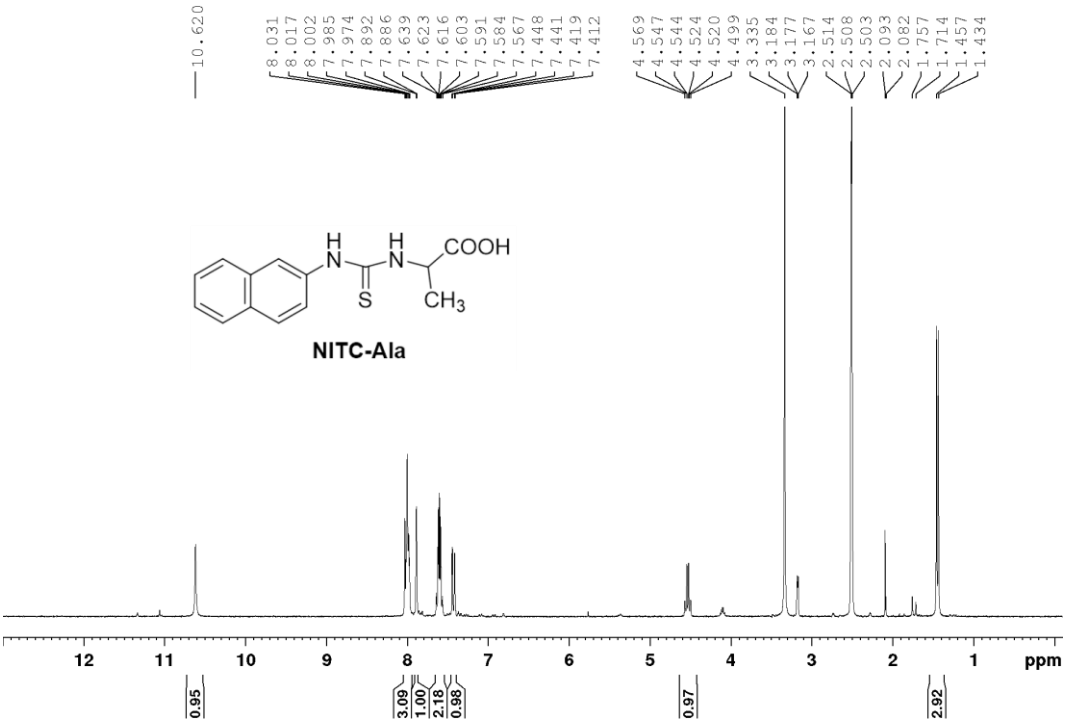

Fig. S24 ^{1}H NMR spectrum of NITC-Ala.

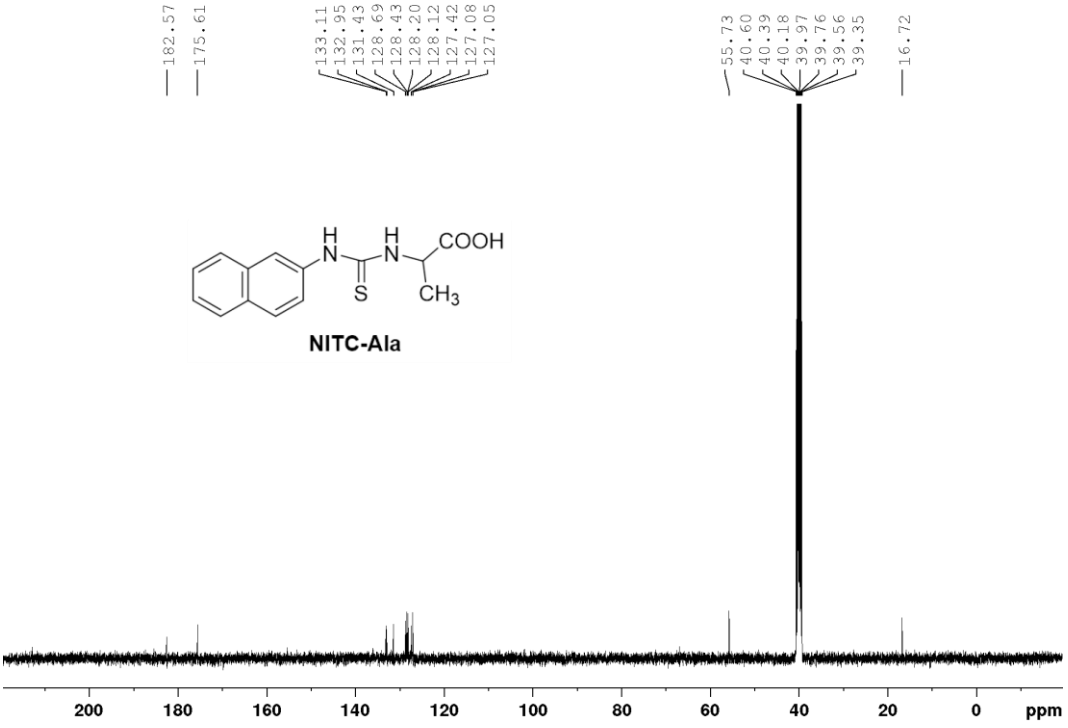

Fig. S25 ^{13}C NMR spectrum of NITC-Ala.

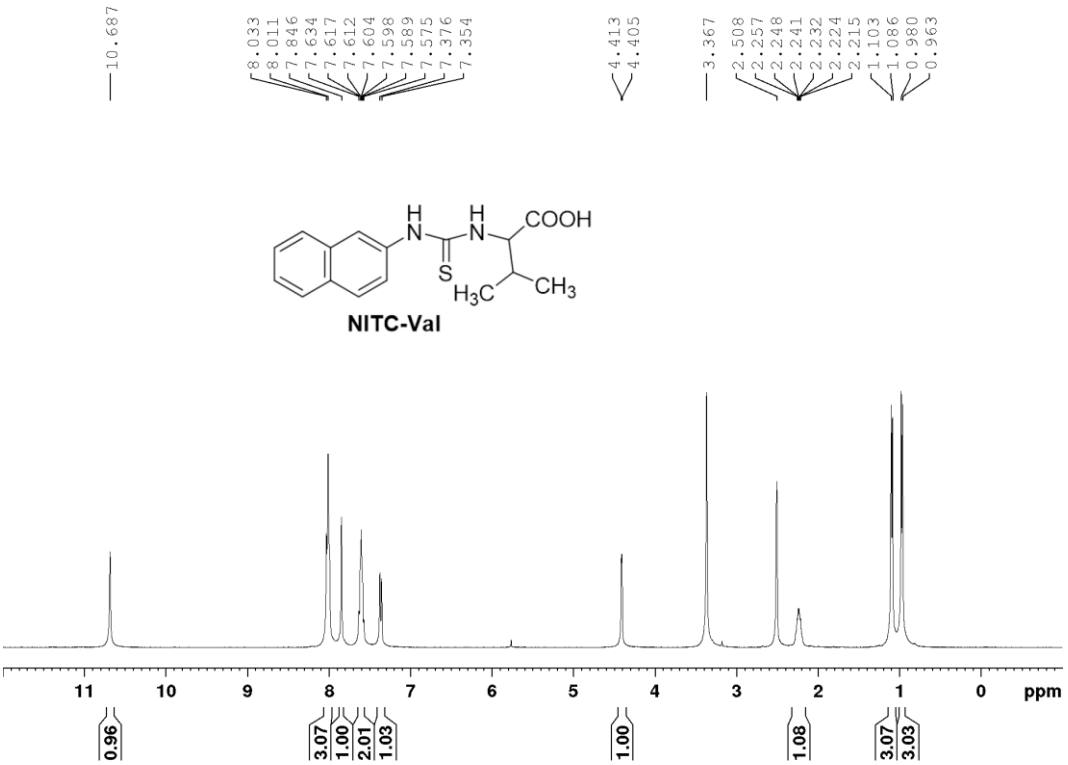

Fig. S26 ^{1}H NMR spectrum of NITC-Val.

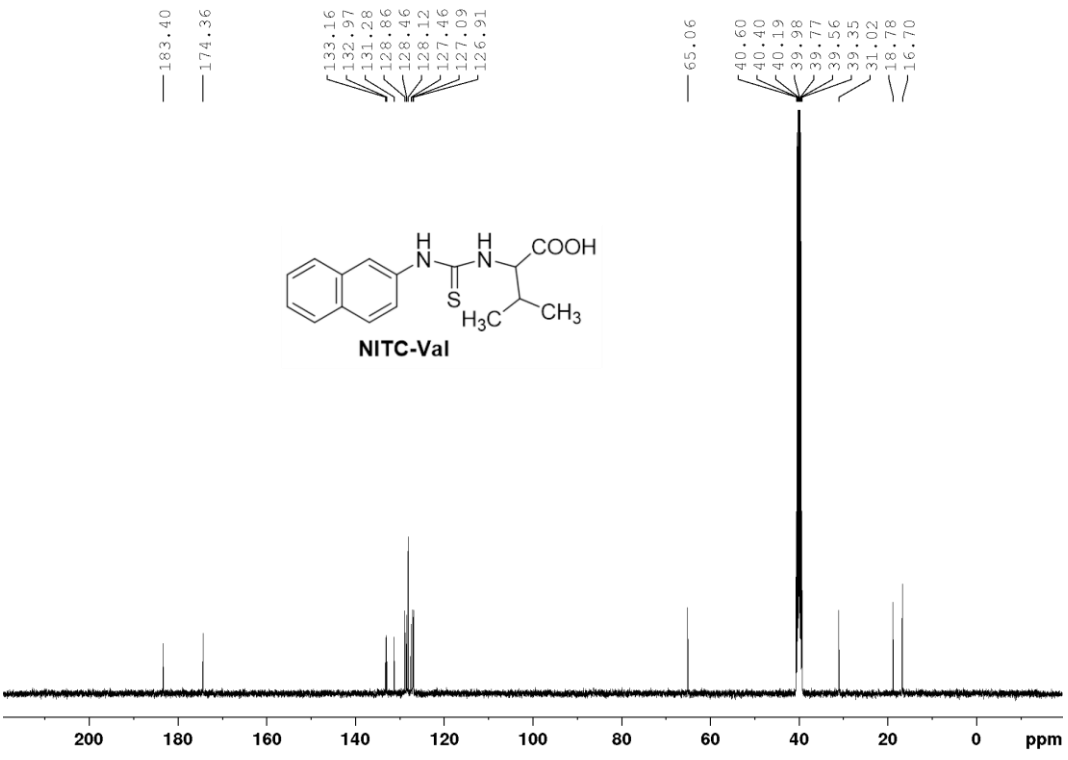

Fig. S27 ^{13}C NMR spectrum of NITC-Val.

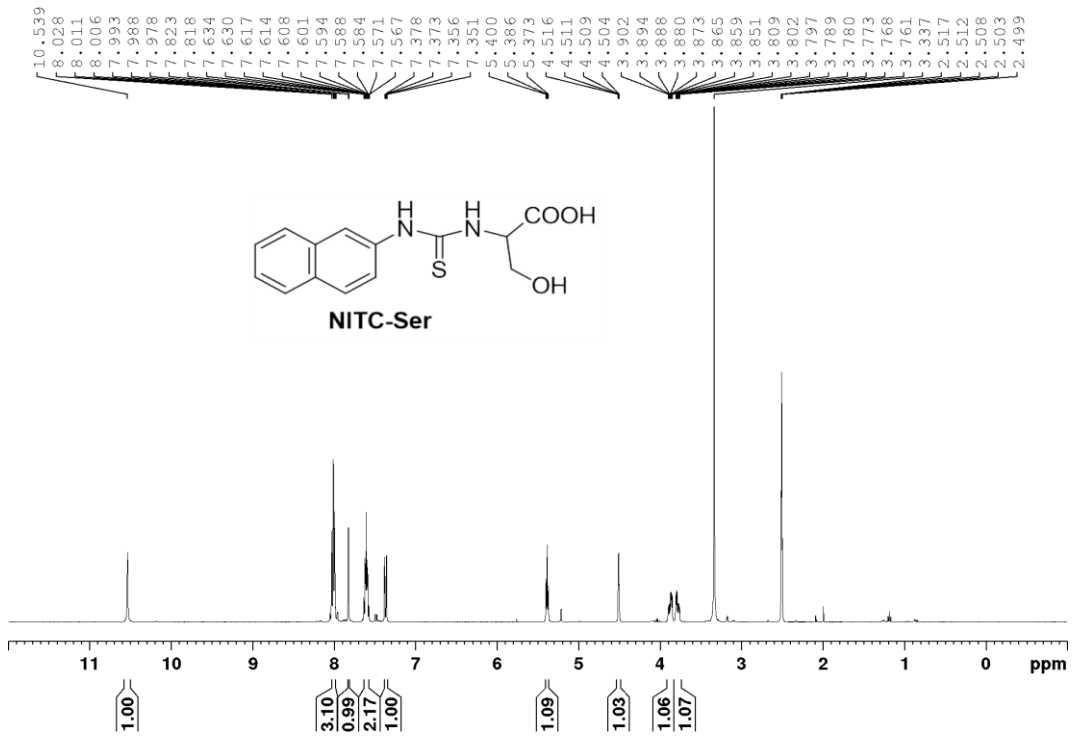

Fig. S28 ^{1}H NMR spectrum of NITC-Ser.

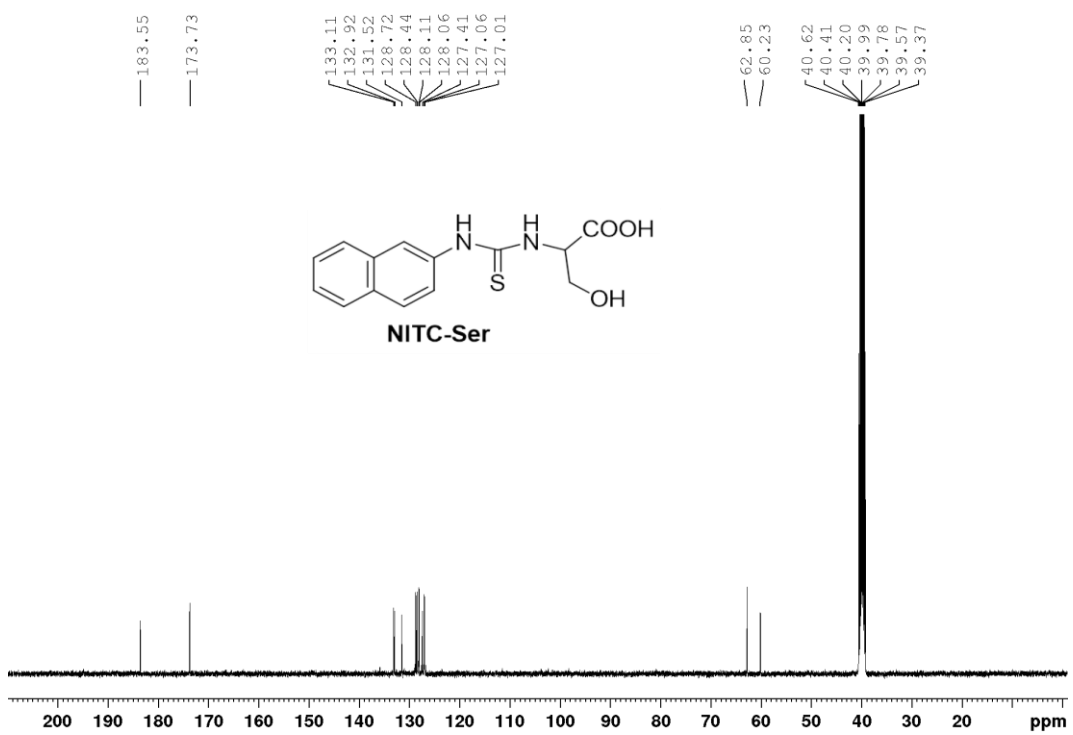

Fig. S29 ^{13}C NMR spectrum of NITC-Ser.

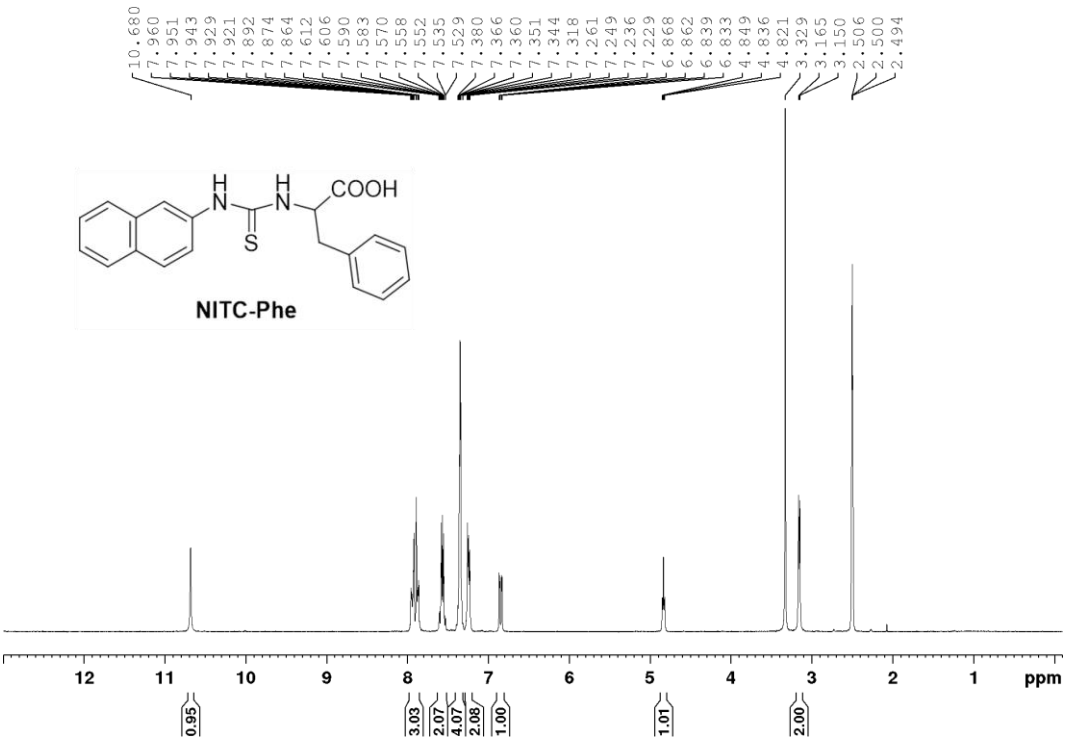

Fig. S30 ^{1}H NMR spectrum of NITC-Phe.

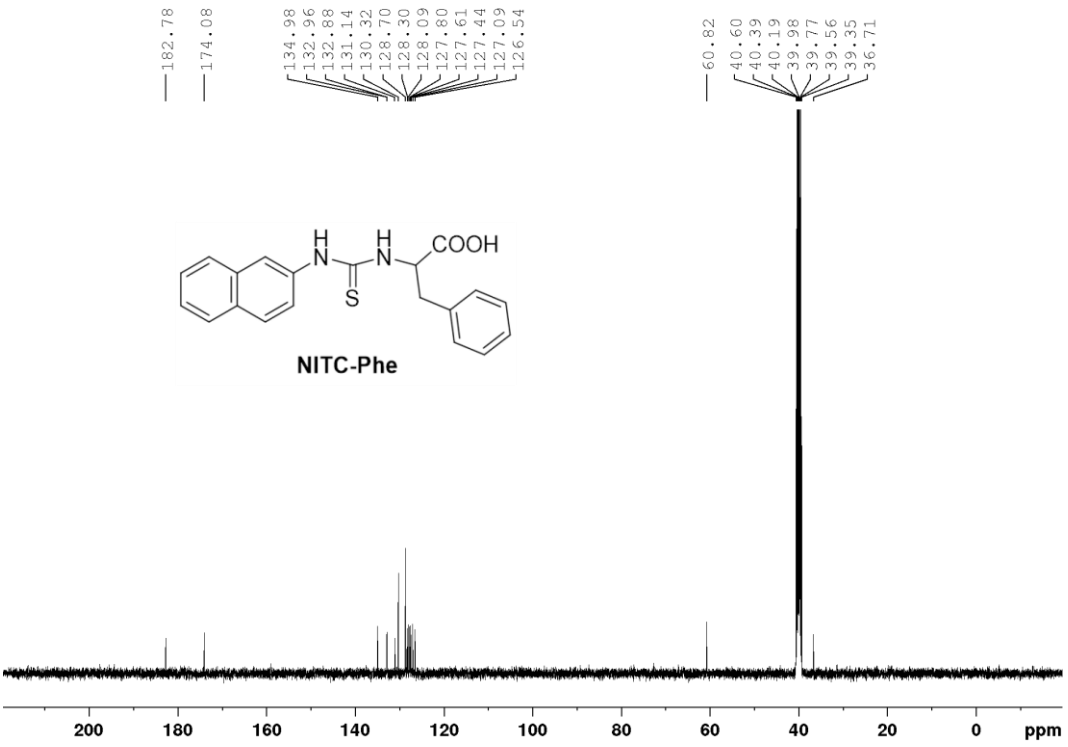

Fig. S31 ^{13}C NMR spectrum of NITC-Phe.

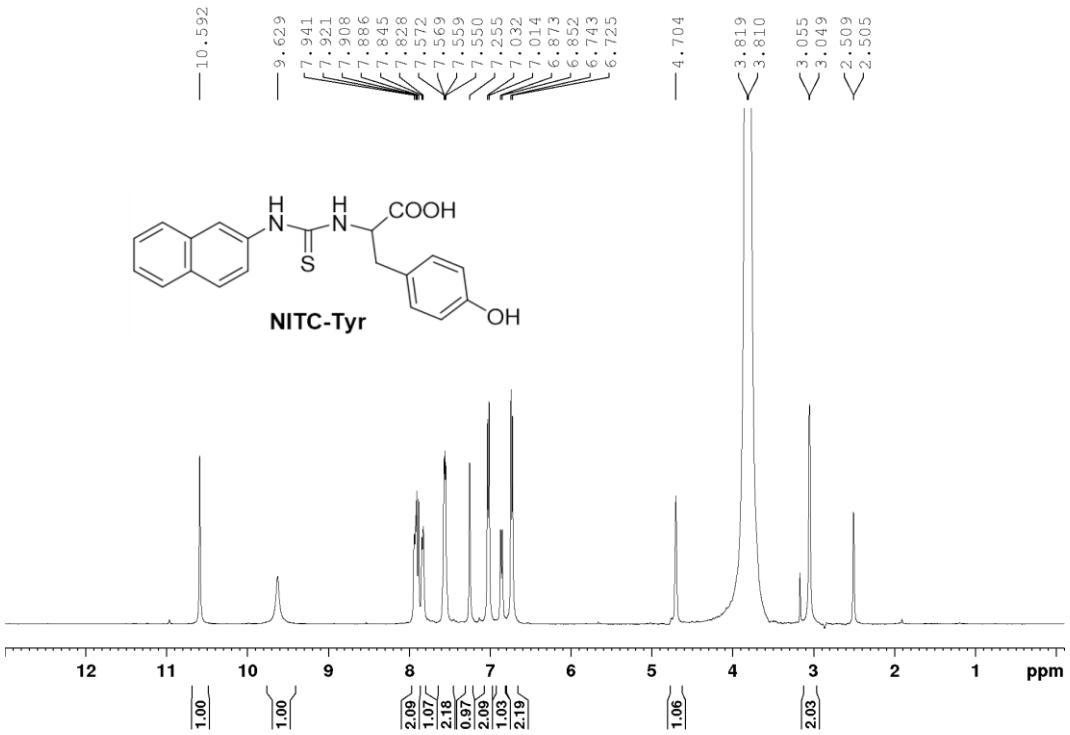

Fig. S32 ^{1}H NMR spectrum of NITC-Tyr.

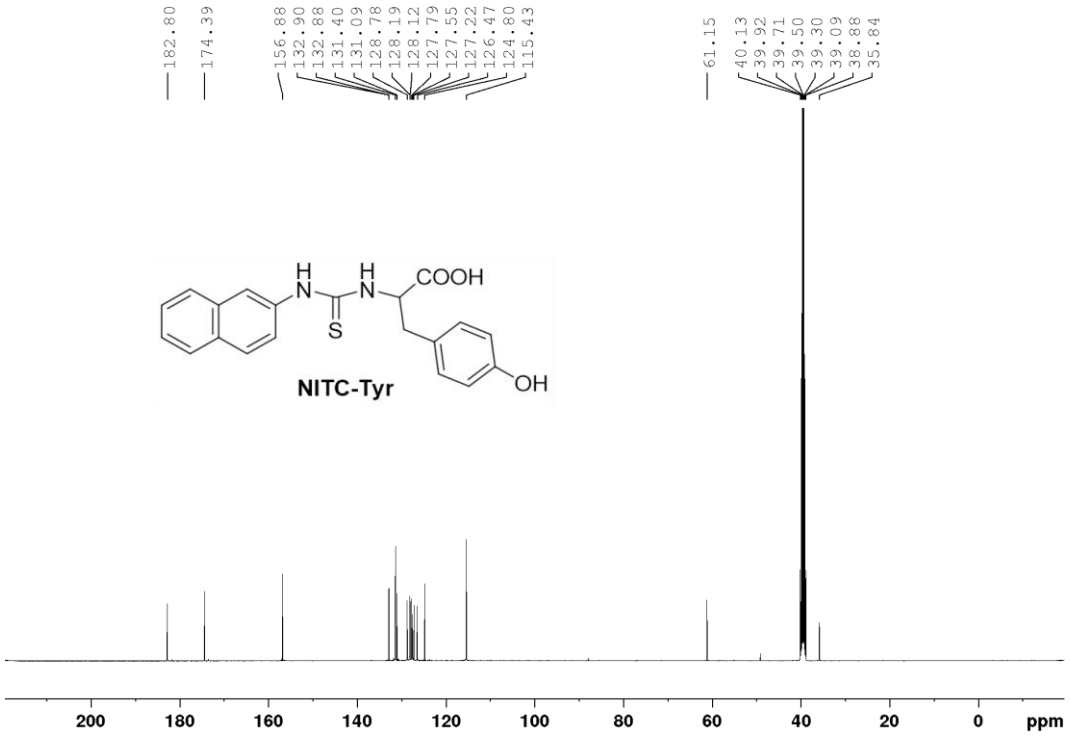

Fig. S33 ^{13}C NMR spectrum of NITC-Tyr.

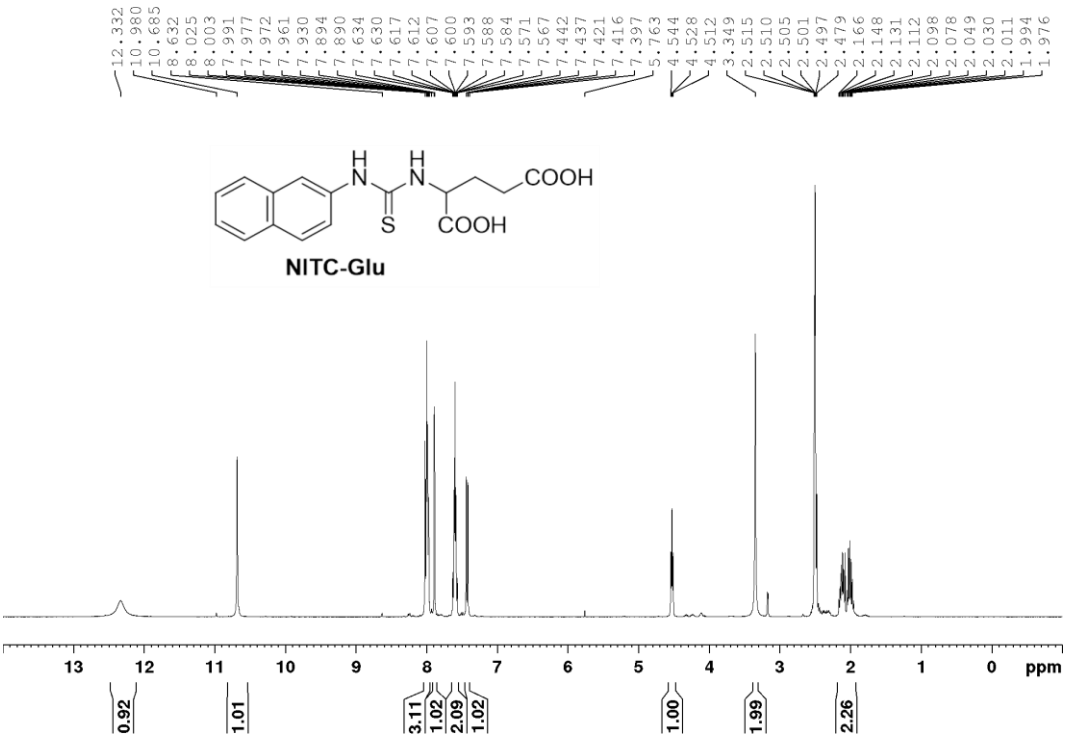

Fig. S34 ^{1}H NMR spectrum of NITC-Glu.

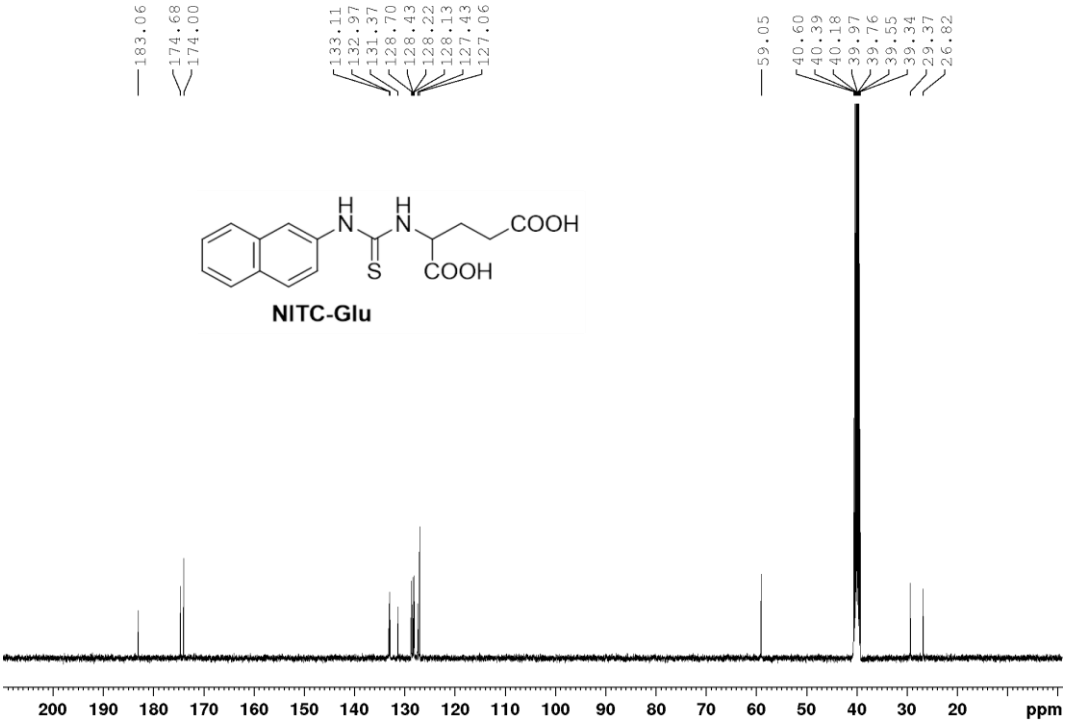

Fig. S35 ^{13}C NMR spectrum of NITC-Glu.

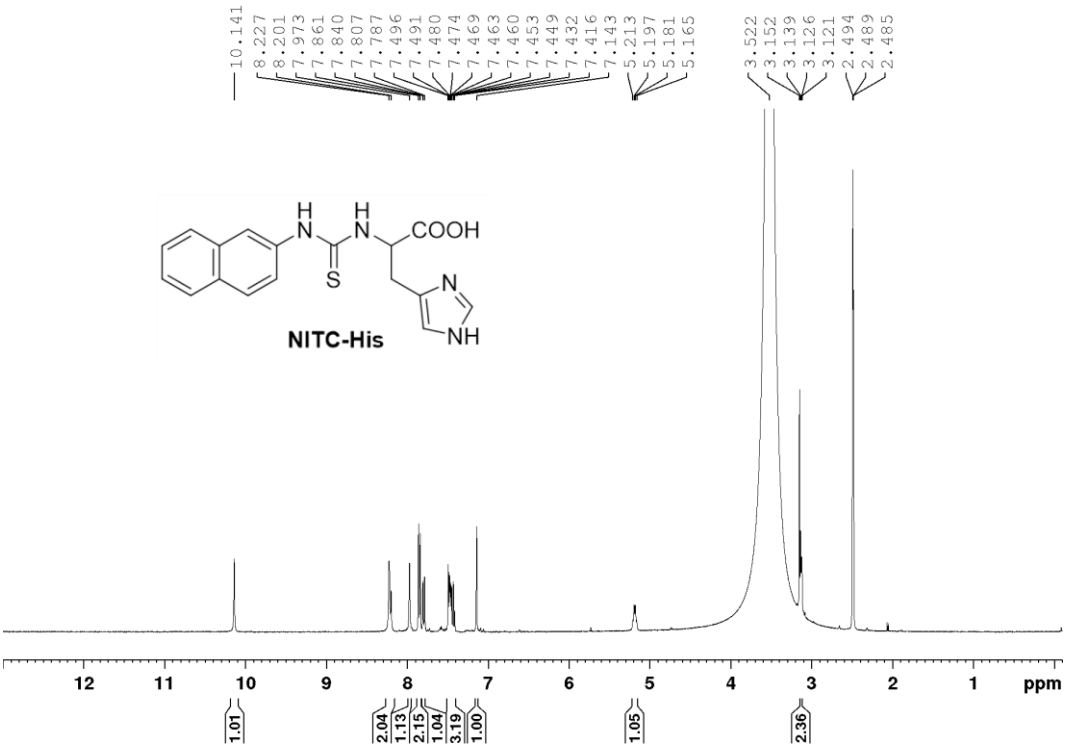

Fig. S36 ^{1}H NMR spectrum of NITC-His.

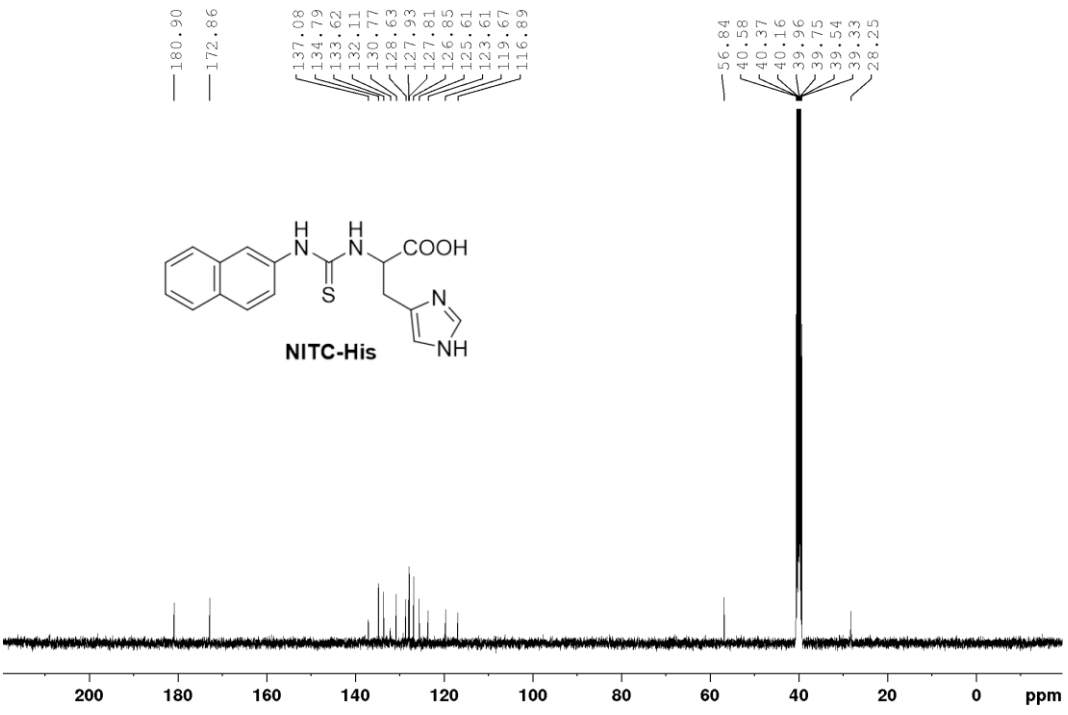

Fig. S37 ^{13}C NMR spectrum of NITC-His.

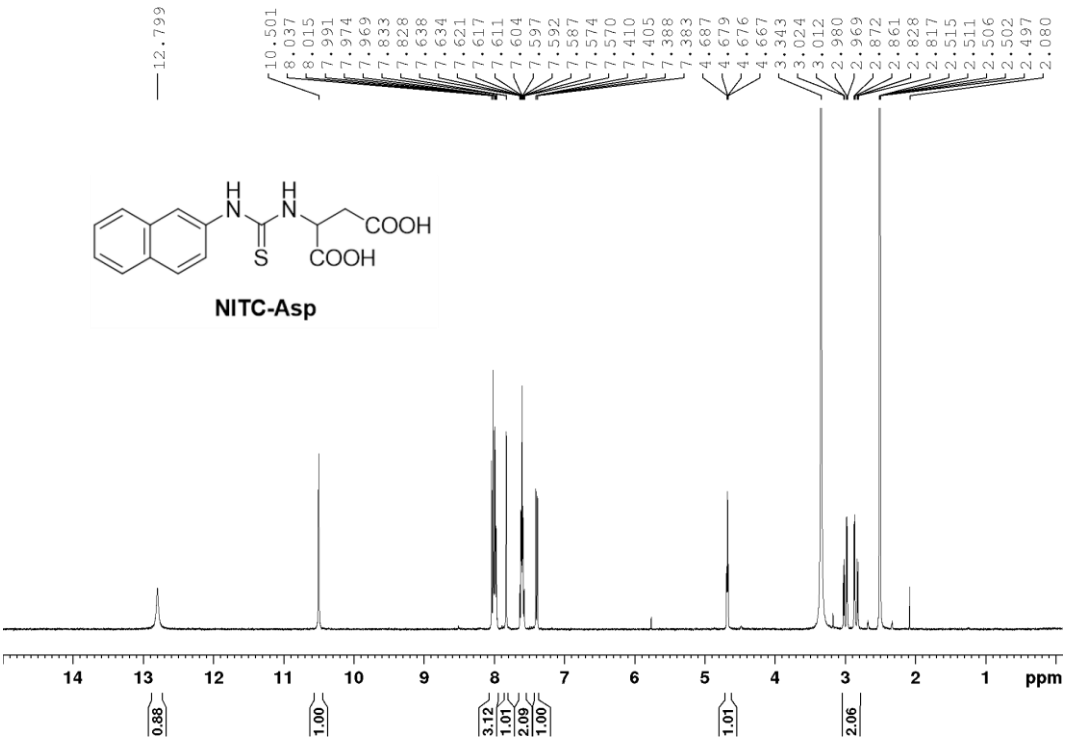

Fig. S38 ^{1}H NMR spectrum of NITC-Asp.

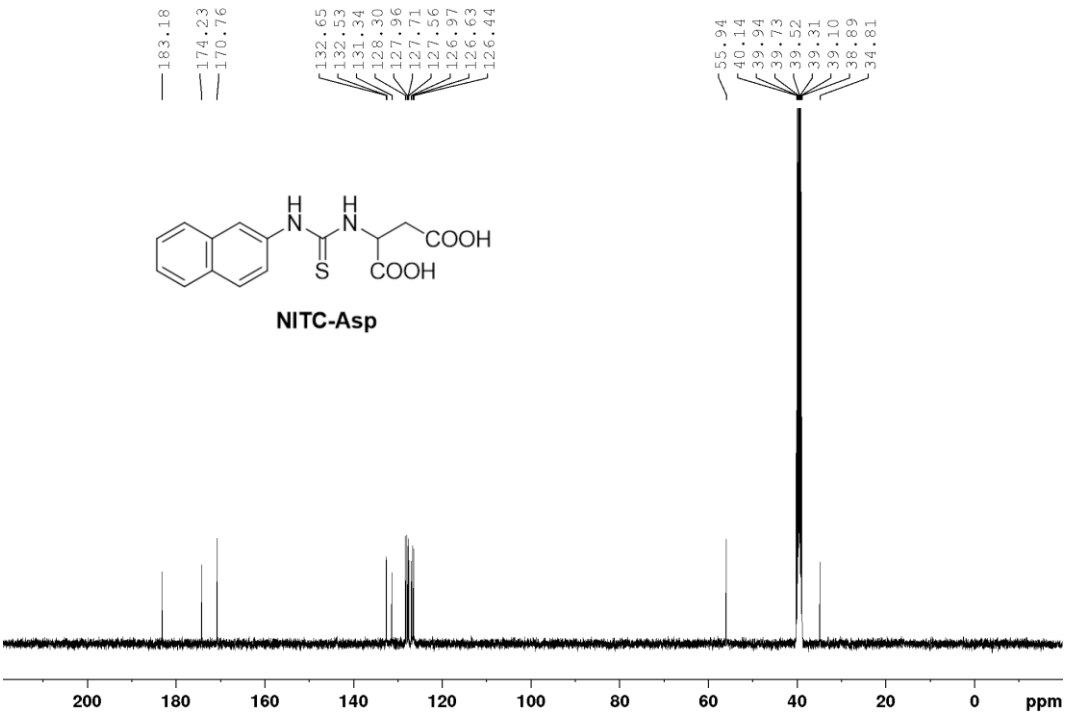

Fig. S39 ^{13}C NMR spectrum of NITC-Asp.